Provenance and tectonic setting of the Paleoproterozoic Denham Formation in east-central Minnesota

Sarah Vorhies

Submitted to the Department of Geology

of Smith College

in partial fulfillment

of the requirements for the degree of

Bachelor of Arts with Honors

John Brady, Faculty Advisor

May, 2006

Table of Contents

List of Figures ii

List of Appendices iv

Abstract v

Introduction 1

- Geologic setting 2
- Rock units and field relations 3
- Possible source rocks 8
- Problem 12

Methods 14

- Zircon dating 14
- Meta-basalt geochemistry 19

LA-ICPMS Results 20

- Sample 05KP30 20
- Sample 05KP32 22
- Sample 05KP36 27

Whole rock geochemistry Results 28

Discussion 32

Conclusions 39

References 40

Appendices

List of Figures

Figure		Page
1	Sample locations	4
2	Stratigraphic column of the Denham Formation	5
3	Geologic map of the Denham Formation	6
4	Geologic map of Minnesota showing location of Minnesota River Valley	9
5	Geologic map of the Minnesota River Valley region	10
6	Map of Minnesota showing locations of greenstone belts	12
7	Frequency histogram of concordant analyses from sample 05KP30	21
8	Inverse concordia diagram of concordant analyses from sample 05KP30	22
9	Frequency histogram of concordant analyses from sample 05KP32	23
10	Inverse concordia diagram of concordant analyses from sample 05KP32	24
11	Frequency histogram of all analyses from sample 05KP32	26
12	Concordia diagram of all analyses from sample 05KP32	27
13	Inverse concordia diagram of all analyses from sample 05KP36	28
14	Plot of wt% SiO_2 versus alkalies in the Denham meta-basalt	29

15	Plot of trace elements Y, La, and Nb in the Denham meta-basalt	30
16	Histogram of concordant analyses from samples 05KP30 and 05KP32 with boxes indicating the ages of possible source regions	37
17	Simplified map of Minnesota showing source region locations in relation to the Denham Formation	38

List of Appendices

A	Bedrock map of Minnesota
B	Table of Samples
C	Table of data from sample 05KP30
D	Table of data from sample 05KP32
E	Table of data from sample 05KP36
F	Table of whole rock geochemistry from sample 05KP33

Abstract

The Denham and Little Falls formations in east-central Minnesota are a Paleoproterozoic sequence of metamorphosed sedimentary and igneous rocks. The purpose of this study was to determine the tectonic setting of the Denham area during the time period of the deposition and the source of the sediments that make up the formation. Laser Ablation-Inductively Coupled Plasma Mass Spectrometry (LA-ICPMS) age dating of detrital zircons extracted from the Denham was used to identify the ages of the sediments that make up the meta-sedimentary rocks. Whole rock geochemistry of major and trace elements was analyzed using X-ray fluoroscopy to determine the tectonic setting responsible for the formation of the meta-basalt that occurs in the middle of the Denham sequence.

The lowest conglomeratic arkose in the sequence yielded 107 analyses that are more than 90% concordant. There are four major groupings of ages at around 2,100 Ma, 2,625 Ma, 2,900 Ma, 3,300 Ma and 3,450 Ma. The youngest zircon grain is 2,072±17 Ma and the oldest grain is 3,447±17 Ma. In the middle of the sequence is a dolomitic arkose which yielded 54 analyses that were more than 90% concordant. The major age groupings are between 2,600 Ma and 2,800 Ma, and between 3,360 Ma and 3,500 Ma. The youngest zircon grain is 2,173±11 Ma and the oldest grain is 3,505±8 Ma. The uppermost schist yielded only one zircon on which two analyses were done. These two discordant ages are 1962±9 Ma and 1929±10 Ma. The meta-basalt has normative plagioclase and orthoclase, diopside, olivine, and nepheline. It has 53% SiO_2 and 7% Na_2O+K_2O. This chemistry makes the basalt part of the alkaline series. Trace elements

also indicate an alkaline composition, which supports a previous hypothesis of a continental rift opening up an ocean basin (Boerboom and Jirsa, 2001).

The age of the Denham can also be constrained by the results. It must be older than the 2,009 Ma cross-cutting dikes (Holm et al., 2005) and younger than the youngest zircon found (2,072.7±17.9 Ma in the lowest sample). Gneisses from the Minnesota River Valley are most likely the sources for the zircons dated between 3,385 Ma and 3,500Ma. There are zircons between the ages of 3,200 Ma and 2,370 Ma that originated in the northern part of the Superior Province. The zircons between 2,963 Ma and 2,740 Ma are from the Wabigoon Greenstone Province. The large groupings of zircons between the ages of 2,650 Ma and 2,750 Ma are from the Kenoran Orogeny and maybe the Wawa Greenstone Subprovince as well. Zircons around 2,100 Ma and 2,200 Ma in younger rocks can possibly be attributed to Proterozoic rocks that we have no current record of (Hemming et al., 1995). There are few zircons with ages near the 2,557 Ma age of the closest gneiss in the area, a very surprising result considering that this is the closest obvious source of sediment for the Denham rocks.

Introduction

The Denham and Little Falls formations in east-central Minnesota are a Paleoproterozoic sequence of metamorphosed sedimentary and igneous rocks. They are both part of the Mille Lacs group. The deposition age of these rocks is unknown but can be constrained to be younger than the 2,557 ±15 Ma unconformably underlying gneiss and older than the 2,009 Ma mafic dikes which crosscut the Mille Lacs group (Holm et al., 2005). Furthermore, a meta-basalt in the Denham formation has a Sm-Nd age of 2,197 Ma (Beck, 1988).

The Denham formation is a small part of the much larger Archean craton known as the Canadian Shield. The Canadian Shield is among the oldest landmasses that preceded the modern continents. Once the information in this study is known, the processes in the area can then be correlated with events that happened in other areas of the craton. This will help create a more complete interpretation of the development of the Minnesota area.

The purpose of this study is to determine the tectonic setting of the Denham area during the time period of the Denham deposition. This is part of a larger undertaking of a 2005 project by the Keck Geology Consortium in which other involved students are determining provenance for rocks across Minnesota and Wisconsin. LA-ICPMS age dating of detrital zircons extracted from the Denham is used to identify the provenance of the sediments that make up the meta-sedimentary rocks. Whole rock geochemistry of major and trace elements measured by X-ray fluorescence spectroscopy is used to determine the tectonic setting responsible for the formation of the meta-basalt that occurs in the middle of the Denham sequence.

Geologic Setting

The Denham and Little Falls Formations lie in east-central Minnesota (Figure 1). This area of the United States is on the southern portion of the Canadian Shield as part of the Superior Province. A detailed bedrock map of Minnesota and surrounding states is included as appendix A. The formations in question were deposited while the Canadian Craton was expanding. The ideas for processes causing this expansion, both here and on other cratons, during the Archean and Paleoproterozoic Eons are still debated, but scientists agree that during this time small cratons and island arcs were colliding and new rock was being formed on these landmasses to create a continental crust that closely resembles that which now exists. There are also debates about whether modern theories of plate tectonics can be used as an analog for Archean tectonic processes, but based upon similarities found in some of the oldest land it appears that the processes were not very different (Windley, 1986, p. 409).

A common rock formed during the continent building is a greenstone. The existence of greenstone belts dated between 2,600 Ma and 3,000 Ma is documented on almost all of the cratons from the Archean. One such greenstone belt, which includes the Ely Greenstone, covers the northern part of Minnesota and reaches to within about 40 miles of the Denham Formation. During this time period (2,700 to 2,600 Ma), the Superior Province was subjected to the Laurentian Orogeny (Ermanovics and Wanless, 1983). Just south of the greenstone belts in Minnesota are slightly younger meta-granite intrusions including the 2,557 Ma McGrath Gneiss that lies unconformably beneath the Denham Formation. This juxtaposition between greenstone belts and quartzo-feldspathic

gneisses is also common on many cratons in the 2,700 to 2,500 Ma. time period (Windley 1986, p. 29).

The Denham rocks have been subject to at least one period of metamorphism since their deposition. The major event is the Penokean orogeny, which affected this area around 1,800 Ma. Compressive stresses in the Penokean orogeny are thought to have been oriented north-south because there is an increase in metamorphism from north to south and because there is a foliation oriented east-west. The Denham rocks underwent amphibolite-facies metamorphism at this time. According to metamorphic monazite dating, the metamorphism occurred with monazite growth at 1,840 and 1,800 Ma (McKenzie, 2004). The two dates found are likely to both be from the Penokean orogeny but different stages of it. There have been other tectonic events in the central United States and Canada since the time of the Denham deposition such as the mid-continent rift, but no other event has affected the Denham as much as the Penokean.

Rock units and field relations

The Denham formation and the underlying McGrath Gneiss outcrop on private property in the town of Denham, MN. The samples were all collected during summer of 2005. Most of the outcrops are small, glacially polished whalebacks. Others are obscured by vegetation and mosses, but provided adequate samples nevertheless. The area was described and mapped by Terrence Boerboom and Mark Jirsa (Boerboom and Jirsa, 2001). They prepared the following stratigraphic column (Figure 2) and geologic map of the area (Figure 3). Not all of the units in the cross section by Boerboom and Jirsa were sampled in this study, because they used drill hole as well as outcrop samples

and the present study is only based upon visibly outcropping rocks. Therefore, some of the stratigraphic units listed in their paper are missing or combined in the current paper.

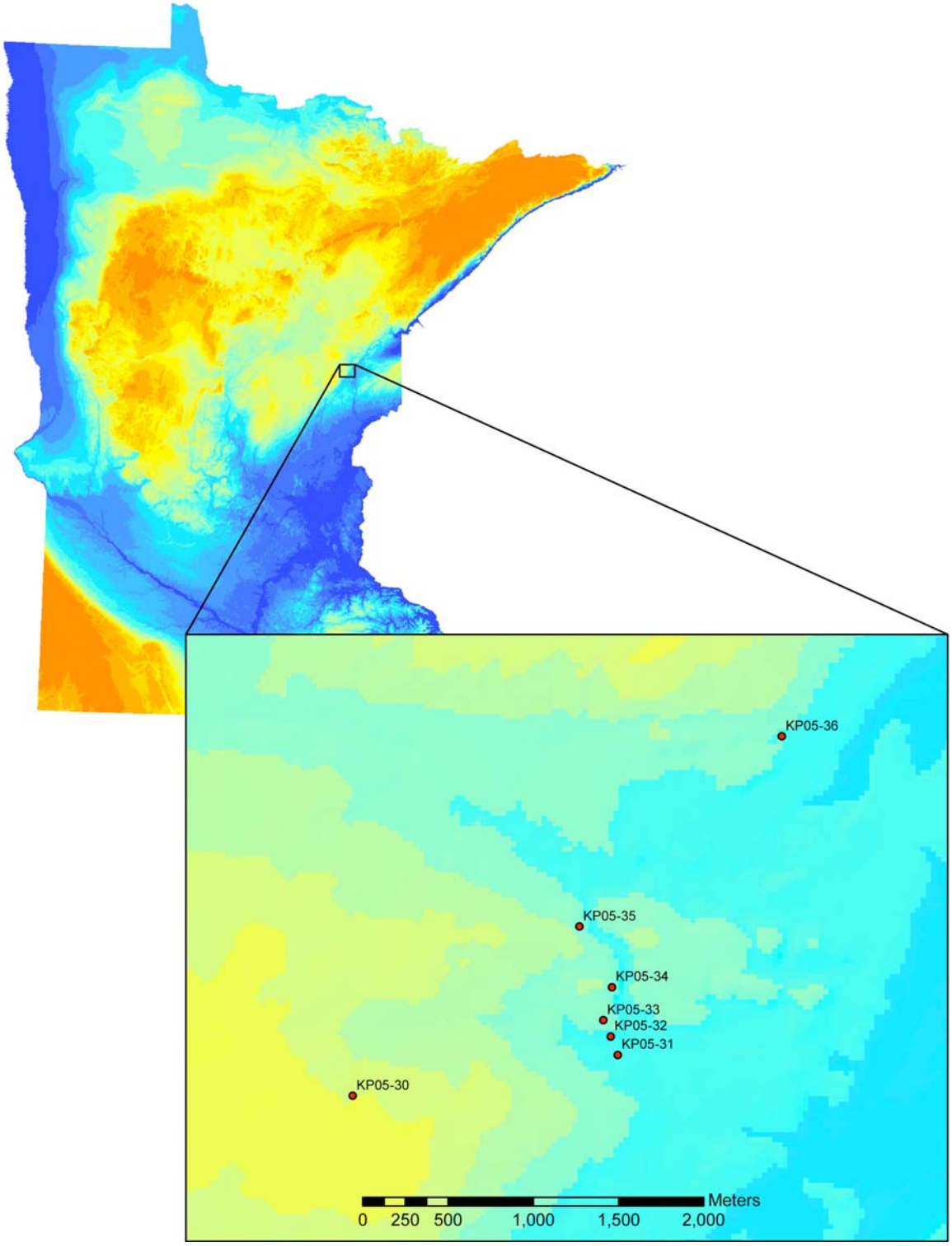

Figure 1: Sample locations on a shaded relief map of Minnesota. Red represents the higher elevations and blue represents the lower elevations.

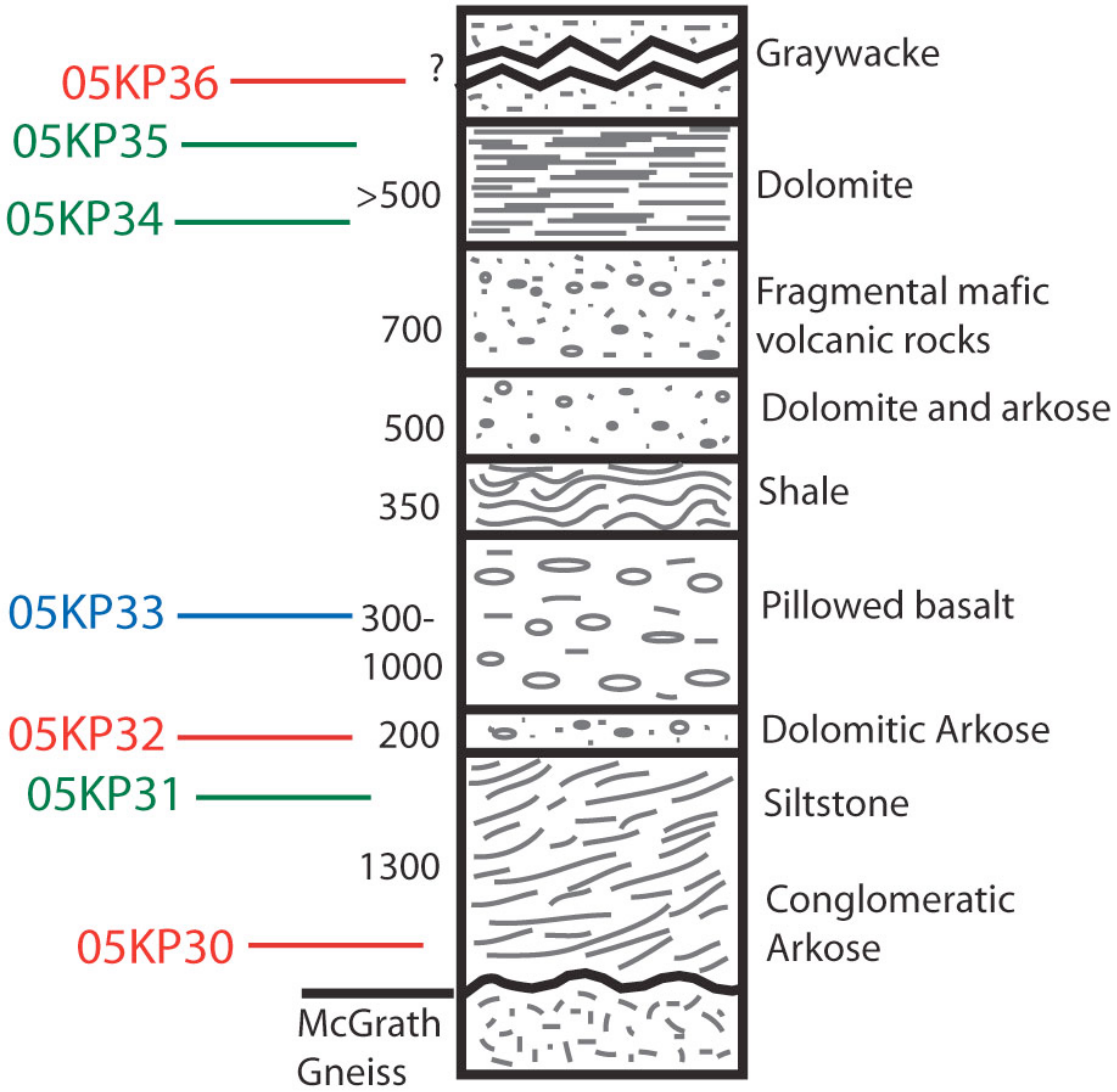

Figure 2. Stratigraphic column of Denham Formation. Locations of samples taken for geochronology are indicated in red, sample taken for geochemistry is indicated in blue, and other samples taken for petrography are indicated in green. Thicknesses in feet. All rocks are metamorphosed, protolith names are given for clarity (modified from Boerboom and Jirsa, 2001).

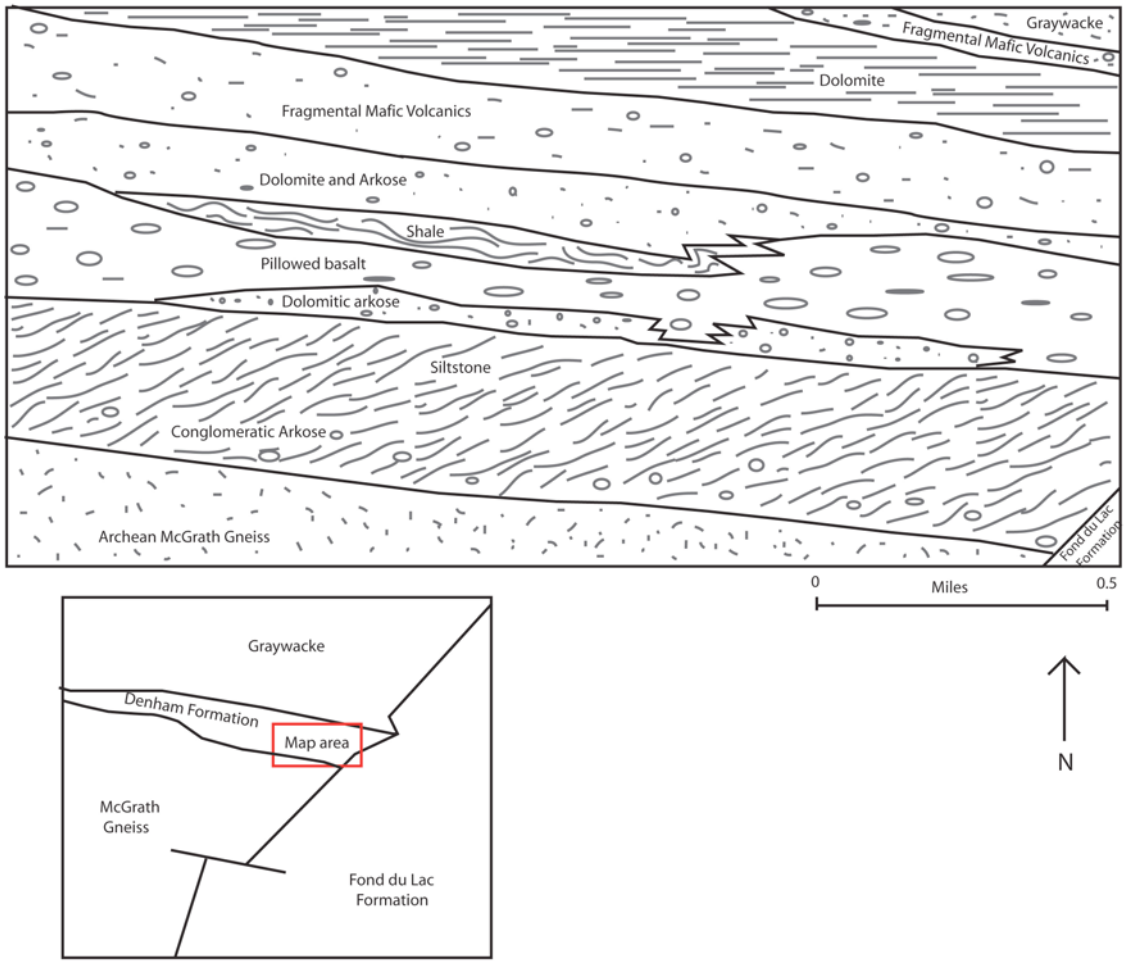

Figure 3. Simplified geologic map of the Denham Formation and the adjacent McGrath Gneiss. All rocks are metamorphosed, protolith names are given for clarity (modified from Boerboom and Jirsa, 2001).

All collected sample locations are marked on a shaded relief map of Minnesota (Figure 1). Data about the samples, including a description, measured bedding and foliation, and UTM coordinates are recorded in the table of samples collected (Appendix B).

The oldest unit within the Denham Formation is an arkose (05KP-30C). It is not very deformed and still shows the original beds and their layering. The beds range from

pebble-sized conglomerates to medium sand-sized arkose. The rock contains about 50% quartz, along with biotite, muscovite, microcline, and albite. Next is a biotite schist (05KP-31) containing biotite, calcite, quartz, muscovite, and microcline. Above that is a calcitic quartzose sandstone (05KP-32) with quartz, calcite, microcline, biotite, and muscovite. The overlying unit is an amphibolite (KP05-33) which has a groundmass of mostly quartz and hornblende with larger (1mm) crystals of calcite. There are many opaque minerals and some plagioclase. This meta-basalt contains remnant pillow structures and is deformed. The final unit of the Denham is a marble sampled in two different stratigraphic locations (05KP-34 and 05KP-35). This rock contains mostly calcite with muscovite and small (1mm wide) quartz veins. The overlying Little Falls formation is located off the Soo Line Trail at Spring Creek road in the town of Denham. The rock present there is a garnet-staurolite schist (05KP-36) that is made up of quartz, garnet, staurolite, biotite, muscovite, and chlorite.

The sediment and basalt sequence that appears to have been present is analogous to that of areas of rifting in more modern times such as the Connecticut River Valley in Massachusetts. The rocks have been metamorphosed but their protoliths can still be identified. The conglomeratic arkose fining upward to a siltstone is interpreted as having been deposited along a shoreline and, as the rift basin deepened, the siltstone was deposited in shallow water below the wave base. The dolomitic arkose was also deposited in a subtidal zone. The basalt that comes next is a common component in rifting and was deposited underwater as evidenced by the pillows. The overlying shale is evidence of further deepening followed by the dolomitic arkose deposited in a shallower subtidal zone. Then there is another deepening indicated by the dolomite that was

deposited in a subtidal zone. Finally there is the Little Falls Schist for which the protolith is a turbidite deposited on a slope in deeper water (Prothero, 2004).

Possible Source Rocks

The first place to look for the source of the Denham sediment is the 2.557 Ga McGrath Gneiss. It is a muscovite-rich, quartzo-feldspathic gneiss with quartz veins. The location of the McGrath can be seen in Figures 2 and 3.

Another possible source region is the Minnesota River Valley subprovince in southwest Minnesota (Figure 4). The rocks found there are the Benson, Montevideo, and Morton block gneisses (Figure 5). These rocks were all dated using thermal ionization mass spectrometry by Schmitz et al. (2006). The Benson rocks were found to be between 2,513 Ma and 2,601 Ma and the Montevideo rocks were approximately 2,600 Ma. This area also includes an intrusion called the Sacred Heart Granite, dated at 2,604 Ma (Bickford et al., 2006) and 2,580 Ma (Schmitz et al., 2006). The Morton Gneiss just southwest of the Sacred Heart Granite has an age of 3,400 Ma. The Minnesota River Valley rocks were also dated using a sensitive high-resolution ion microprobe by Bickford et al. (2006). They found the Montevideo block and the Morton block to have crystallized at 3,500 Ma with an unknown zircon forming event between 3,440 and 3,420. They dated the intrusion of the Sacred Heart Granite at 2,604 Ma. According to Bickford, there are ages of about 2,600 Ma for the Morton and Montevideo rocks that are rims that grew during metamorphism and not primary crystallization ages.

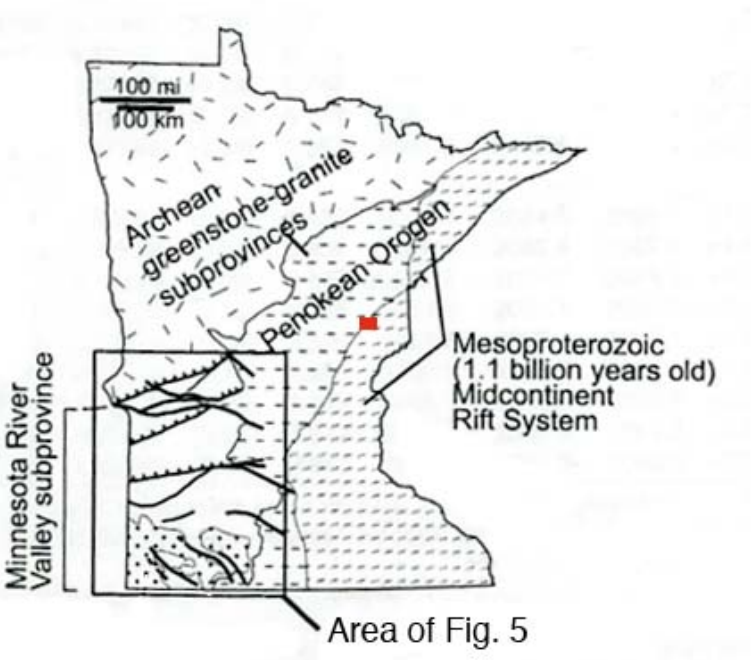

Figure 4: Generalized geologic map of Minnesota showing the location of the Minnesota River Valley with the study area in red (modified from Schmitz et al. 2006).

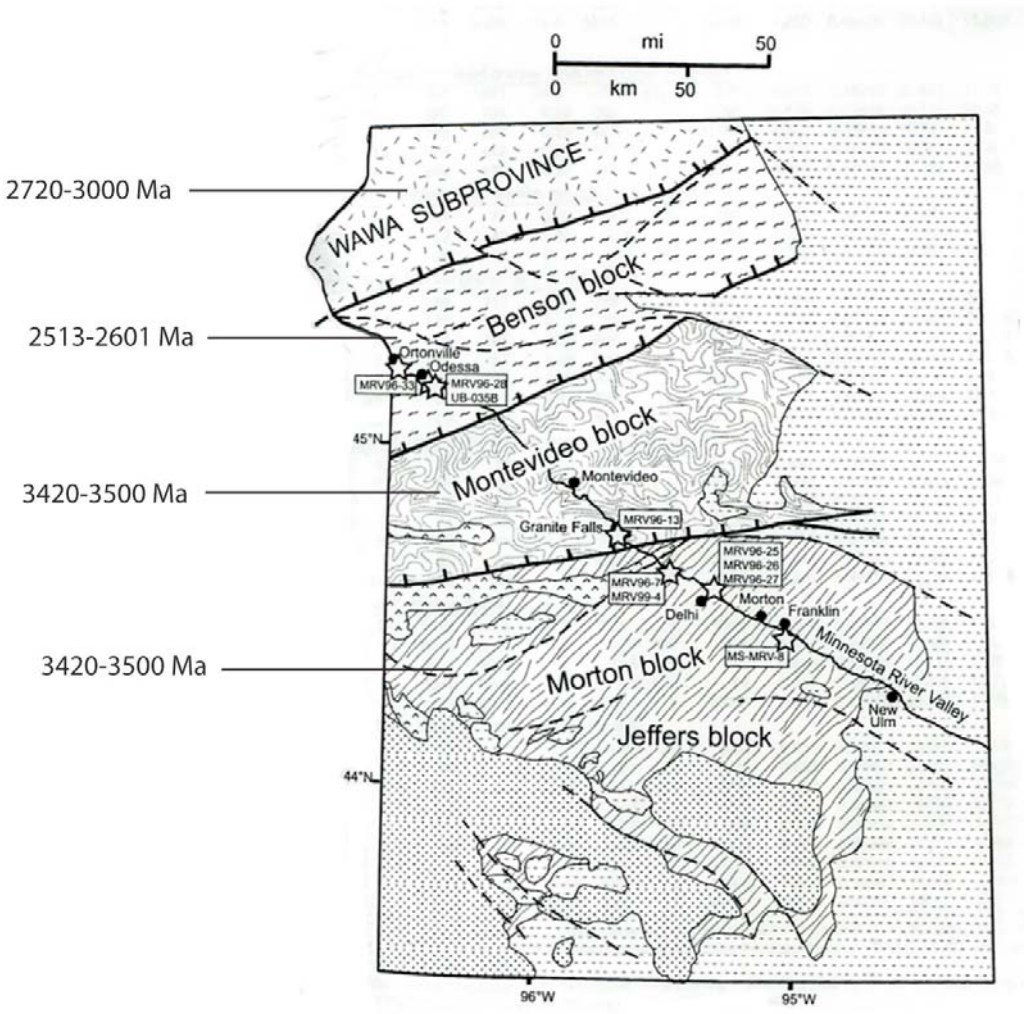

Figure 5: Larger scale geologic map of the Minnesota River Valley region (modified from Schmitz et al., 2006).

There are also numerous greenstone belts in northern and northwestern Minnesota and continuing into Canada (Figure 6). The belts are named by region. The southernmost belt is the Wawa (Abitibi) Volcanic Superbelt that covers most of north-central Minnesota. Next are the Quetico Gneiss Superbelt and the Wabigoon Volcanic Superbelt. There are more belts further north into Canada, but these are likely too far away to have contributed sediment to the Denham formation. The greenstone is

metamorphosed basalt, which likely came from rifts on the sea floor. The Wawa subprovince includes ages between 2,701 Ma and 2,720 Ma. The Wabigoon subprovince includes ages of 2,740 Ma and between 2,898 Ma and 2,963 Ma (Tomlinson and Condie, 2001). Another study dated the Wabigoon Subprovice as having lasted until 2,250 Ma (Ermanovics and Wanless, 1983). The tectonic setting that created these rocks is unknown. While there are possible modern analogues to the formation of these rocks, it is difficult to justify using modern tectonics to model continental movement in the Archean. It is unknown what lies beneath these greenstones, but the older gneiss superbelts found to the south of the greenstones (such as the Morton and Montevideo) might continue further north underneath them (Ojakangas and Matsch, 1982 p. 26).

Another possible source of sediment is from the Kenoran Orogeny, which occurred between 2,650 Ma and 2,750 Ma. This event included volcanism, intrusion of plutons, metamorphism, folding, and faulting and created new rock and terrane in Northern Minnesota and throughout the rest of the Superior Province (Ojakangas and Matsch, 1982 p. 32). Finally there is a region in the northern part of the Superior Province that consists of gneisses and metamorphosed rocks. The dates found there are 3,190 Ma, 3,250 Ma, 3,370 Ma, and many above 3,500 Ma (Bohm et al., 2000). This is a less likely area because of the distance from the Denham formation, but it accounts for the possibility of zircons older than 3,000 Ma.

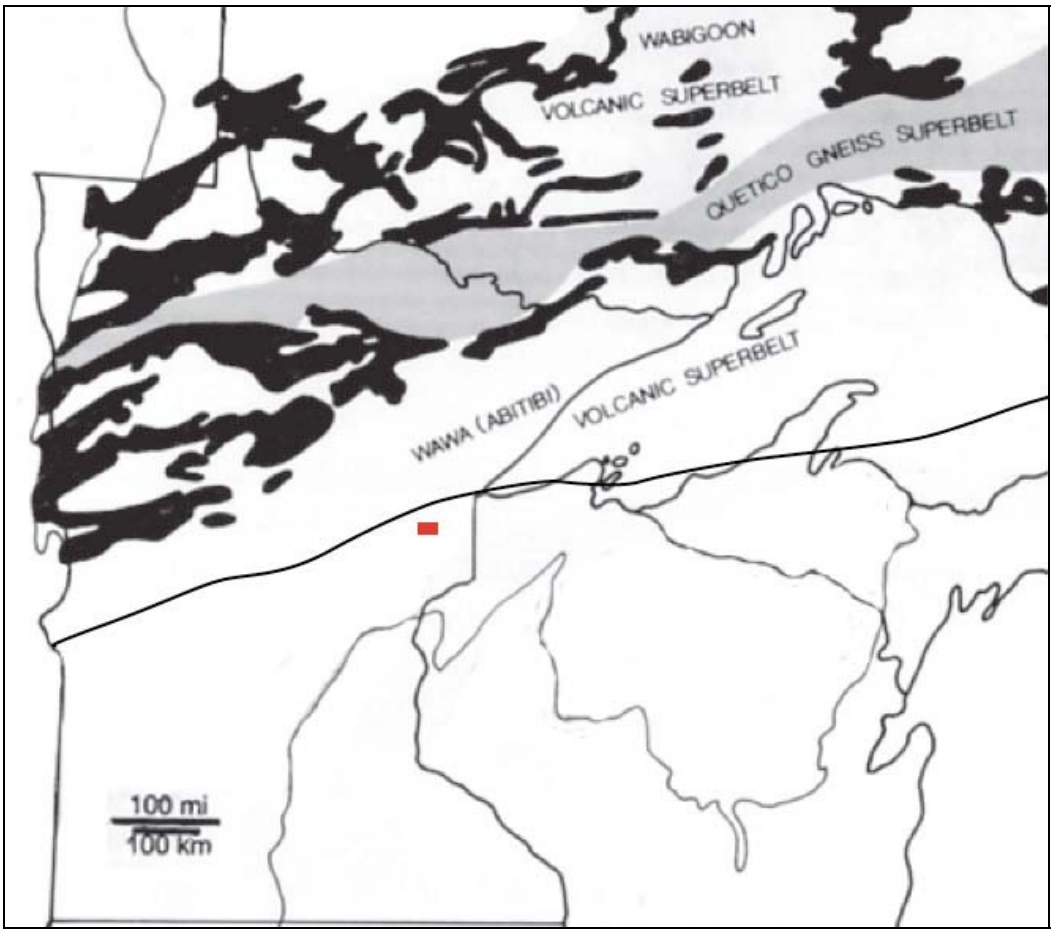

Figure 6: Map of Minnesota and surrounding areas showing locations and names of greenstone belts and the study area in red (modified from Ojakangas and Matsch, 1982 p. 26).

Problem

The area in question has been the subject of few studies. The same can be said for this time period in Minnesota's history. I hope to shed some light on the tectonic processes taking place at this time by studying the provenance and environments of deposition of the Denham and Little Falls Formations. Previous studies have presented hypotheses for the tectonic processes responsible for the rocks in the Denham area.

Thurston (2002) wrote that after the Kenoran Orogeny (~2,700 Ma), the Superior Province was part of the supercontinent Kenorland until lithospheric stretching at 2,480 Ma broke this supercontinent apart. During the aftermath of this breakup (between 2,450 and 2,110 Ma.) there were many intracratonic and continental margin basins created across the Canadian Shield, so it is possible that the Denham sequence is related to these events (Aspler et al., 2001). The time frame given in this scenario correlates with the age range of the Denham and Little Falls Formations. Additionally, the sediment and basalt sequence that appears to have been present is analogous to that of other areas of rifting in more modern times (Boggs, 2001). Boerboom and Jirsa (2001) also wrote that the Denham rocks "represent a rift-margin assemblage" and describe a model of intracratonic rifting where the McGrath Gneiss eroded into an evolving shallow sea. The Denham units appear to have protoliths that most likely represent the deepening of this sea, as well as volcanism produced by the rifting. The methods to be used in this study are U-Pb zircon dating for the meta-sedimentary rocks in the formations, as well as major and trace element geochemistry of the meta-basalt. These data are used to make a more concrete proposition for the tectonic setting.

Methods

Zircon dating

The primary data for the provenance study are the age dates of detrital zircons. Three samples from the stratigraphic column were collected for zircon separation. These are the lowest conglomeratic arkose (05KP-30C), the middle dolomitic arkose (05KP-32), and the upper Little Falls schist (05KP-36). The Little Falls Schist yielded only one zircon after separation techniques were performed, so limited data are available from it. The other two samples give a range of zircon morphologies and ages. 106 zircons were extracted from sample 05KP-32. 120 zircons were extracted from sample 05KP-0C. These will be used to get a picture of the origin of, and the path taken by, the sediments before they became the rocks in the Denham Formation.

In order to perform the laser ablation analyses on zircons from the rocks samples, individual zircon crystals first had to be separated from the rocks. The following procedure is standard for zircon separation as described by many authors including Keith Sircombe (2002). Approximately 80 pounds of each sample were collected. The weathered and altered rinds of the samples were removed and the rock was broken down into pieces no larger than 8 cm in diameter. These cobbles were broken down further by a "Braun Chipmunk", whose steel plates crush the rock into pieces. Next a disc mill was used to grind the pieces into fine sand. At this point the rock has, for the most part, been broken down into individual grains of different minerals.

Zircons are relatively dense minerals with a specific gravity of 4.6 to 4.7. The "Whifley Table" takes advantage of this fact. It shakes back and forth and while directing a constant flow of water at the samples. The result is that the light minerals are

carried off into one of two buckets on the side of the table and the heavier minerals go into one of five different tubs at the end. These five tubs are labeled A, B, C, D, and E, with tub C in the middle where the heaviest of the minerals go.

Magnetic minerals are also very dense, so these ended up in the tubs along with the non-magnetic heavy minerals. There were also many iron filings that came from the disc mill. To get these out of the sample free fall magnetic separation was used. Once again using the zircons' high density, the non-magnetic portion of the sample was put into a heavy liquid (methylene iodide, specific gravity 3.33), where the zircons would sink but few other things would. This material was rinsed with acetone and set under heat lamps to dry.

There were many people working in the lab during sample preparation, therefore in between each step the equipment used was cleaned twice. This reduces the risk of zircons and other minerals from one sample contaminating another sample.

In this study, Laser Ablation-Inductively Coupled Plasma Mass Spectrometry (LA-ICPMS) was used to determine age dates for the detrital zircon grains. This is a common procedure for studies with large numbers of zircons or other minerals to be analyzed. Laser ablation (LA) is an efficient way to transport material for analysis from the mineral for Inductively Coupled Plasma Mass Spectrometry (ICPMS). A detailed explanation of the data collection and reduction techniques can be found in Chang et al. (2006). In this method a laser is used to irradiate an area on a zircon to create a pit on the surface. The laser was fired at 5 Hz with a pit size of 30 microns. The material extracted from the zircon is carried by argon gas to the ICPMS. In the ICPMS the material is ionized and transmitted to the mass analyzer where the isotopes are detected (Feng et al.,

1993). Because of the ability to focus a laser on a very small (30-60 micron) spot on the mineral, in this case a zircon, microscopic analyses can be performed without requiring the lengthy sample preparation that is needed in older techniques (Kosler et al., 2002). The specific equipment used in this study is a Finnigan Element2 High Resolution ICP-MS coupled with the New Wave UP-213 laser ablation system located at Washington State University. The university claims accuracy and precision of 2-3% (Chang et al., 2006). Ages are determined by three different ratios measured by the equipment. The major isotopes that are measured in each zircon are: ^{206}Pb, ^{207}Pb, ^{235}U and ^{238}U. The age of the zircon is determined with three ratios of these isotopes: $^{207}Pb/^{206}Pb$, $^{206}Pb/^{238}U$, and $^{207}Pb/^{235}U$.

Prior to the laser ablation of the zircons, cathodoluminescence images were taken of the individual grains in order to determine where there is zoning and overgrowths. Because the zircons in this study have been metamorphosed, there may be many multiple age zones (Faure 2001, p. 19). The age of the outermost zone of the zircon is that which this study is concerned with because that will be the age of the last major event to which the zircons were subjected. While there was some post lithification metamorphism, zones that result from this are generally too small to be dated by this technique.

Feng et al. (1993) performed one of the first experiments using LA-ICPMS to ascertain $^{207}Pb/^{206}Pb$ ages of zircons. They used zircons that had previously been dated using thermal ionization mass spectrometry (TIMS) to examine the accuracy, precision, and limitations of the LA-ICPMS technique. It was found that the precision of the Pb ratio is about .5-6% depending on the lead concentration in the zircon and on fluctuation of the signals. Their suggestion for a solution to the signal fluctuation was to have an

increased number of signals with shorter acquisition time. In comparison to TIMS results, the zircons dated were almost completely within 2% concordance (Feng et al., 1993).

When the article was written in 1993, Feng et al. reported that the LA-ICPMS had not yielded very precise U/Pb ratios and so was not considered as good as other methods such as SHRIMP (Sensitive High Resolution Ion MicroProbe). Also in 1993, however, Fryer et al. reported results for U/Pb dates in zircons that were not statistically different from those calculated by other methods. There is a more precise method for zircon U-Pb isotope dating called secondary ion mass spectrometry (SIMS). SIMS also has its other advantages including the fact that there is no laser ablation so there is less damage to samples. For this project, however, LA-ICPMS is arguably better because it is less costly and faster. Because this provenance study needs to analyze many different zircon grains from each rock sample, being able to do so quickly is advantageous (Kosler et al., 2002). This is the only analysis that the zircon samples are being used for so the damage to them is inconsequential.

Once the range of ages of zircons is learned, they are put into major age groups represented in the sample. These can be compared to the ages of older rocks in the area being studied. If a group of zircons all resulted in a similar age date and also have similar morphologic characteristics, it can be assumed that they all originated in the same rock. The statistical methods of this are described in Andersen (2005). He asserts that the use of a small number of zircon dates to extrapolate the provenance processes is problematic because, based upon his statistical modeling, it is unlikely that the data will give precise or accurate impression of the age distribution of the rock. He says however that as long

as there are at least 70 randomly chosen grains and 120 total grains this error should be minimized. This study dated 120 zircons from sample 05KP-30 and the available 106 from 05KP-32 and they were all chosen randomly. An additional use of the zircon ages is to give a youngest possible age of deposition for the rock being studied. While the difference between the zircon's age and the date of deposition may be off by even billions of years in some cases, the youngest zircon in the sample should be no older than the age of deposition (Andersen, 2005).

A total of 120 grains from sample 05KP-30, 106 grains from sample 05KP-32 and 1 grain from 05KP-36 were analyzed. A few grains in each sample were large enough or had distinct enough zoning to warrant multiple ablation spots and analyses on the same grain. Some of the analyses had to be rejected or labeled as suspect based upon certain criteria. Any analysis for which all three isotopic ages calculated are more than 90% concordant is considered a good analysis and a reliable age date. Because the ICPMS takes 300 measurements, there is room to remove the outliers and sections of the sweep that looked like questionable. If parts of the analysis did not look right, for example if the pattern of measurements taken throughout the scan was such that the laser appeared to have fired through different zones or even through the entire zircon and into the epoxy, the measurements were removed from that analysis. If too many of the measurements were removed to get a reliable $^{206}Pb/^{238}U$ intercept, the age was only taken from the $^{207}Pb/^{206}Pb$ average. These analyses are not necessarily as accurate, but are still worth examining. In most cases the grains that provided only good $^{207}Pb/^{206}Pb$ ages or were less than 90% concordant were not very far off of the grains whose ages were concordant. When possible, all ages were included in analysis to make the data more

robust. Once the sample results were reduced the ages that were more than 90% concordant were plotted on frequency histograms and Concordia diagrams.

Meta-Basalt Geochemistry

A sample of the amphibolite (05KP-33) was also taken for major and trace element geochemistry analysis. The protolith of the amphibolite is basalt, which can occur in many different depositional environments and tectonic settings. While the general name basalt is found in all of these environments, it is not the exact same magma that is extruded. The major and trace element whole rock geochemistry is different depending upon the circumstances. By comparing the results for the geochemistry of the Denham amphibolite to the values determined for other types of basalts, a conclusion can be made regarding the tectonic setting responsible for the Denham basalt. Beyond the assessment of tectonic setting, a conclusion can also be made more specifically about the magma chamber from which the magma originated and the amount of crustal contamination or a plume origin. It is probable that the geochemistry will indicate or be compatible with the continental rift hypothesis of Boerboom and Jirsa (2001), but the analysis has never been done.

Whole rock geochemistry of the meta-basalt in the Denham sequence (05KP-33) was performed using the X-Ray Fluorescence Spectrometer at Macalester College. Glass beads were used to determine major elements and pressed powders were used to determine trace elements.

LA-ICPMS results

Sample 05KP30

From this sample 120 grains were analyzed one or more times resulting in 129 total analyses. Of these 107 are more than 90% concordant, 21 are less than 90% concordant, and 1 was culled. The concordant samples are those with the least error and are therefore the focus of study. Of the concordant samples the youngest zircon grain is 2,072±17Ma. The oldest grain is 3,447±17Ma. A spreadsheet with all the analyses is included as appendix C. There are four major groupings of ages at around 2100 Ma, 2,625 Ma, 2,900 Ma, 3,300 Ma and 3,450 Ma. These groups of ages are shown on Figure 7, a frequency histogram of the more than 90% concordant zircons' ages. Figure 8 is a concordia diagram for this sample that includes only those grains that are more than 90% concordant. For this sample, since there were 107 analyses (an adequate number) that are more than 90% concordant, the discordant analyses were not examined more closely. This is not the case with the following sample as will be explained later in this section.

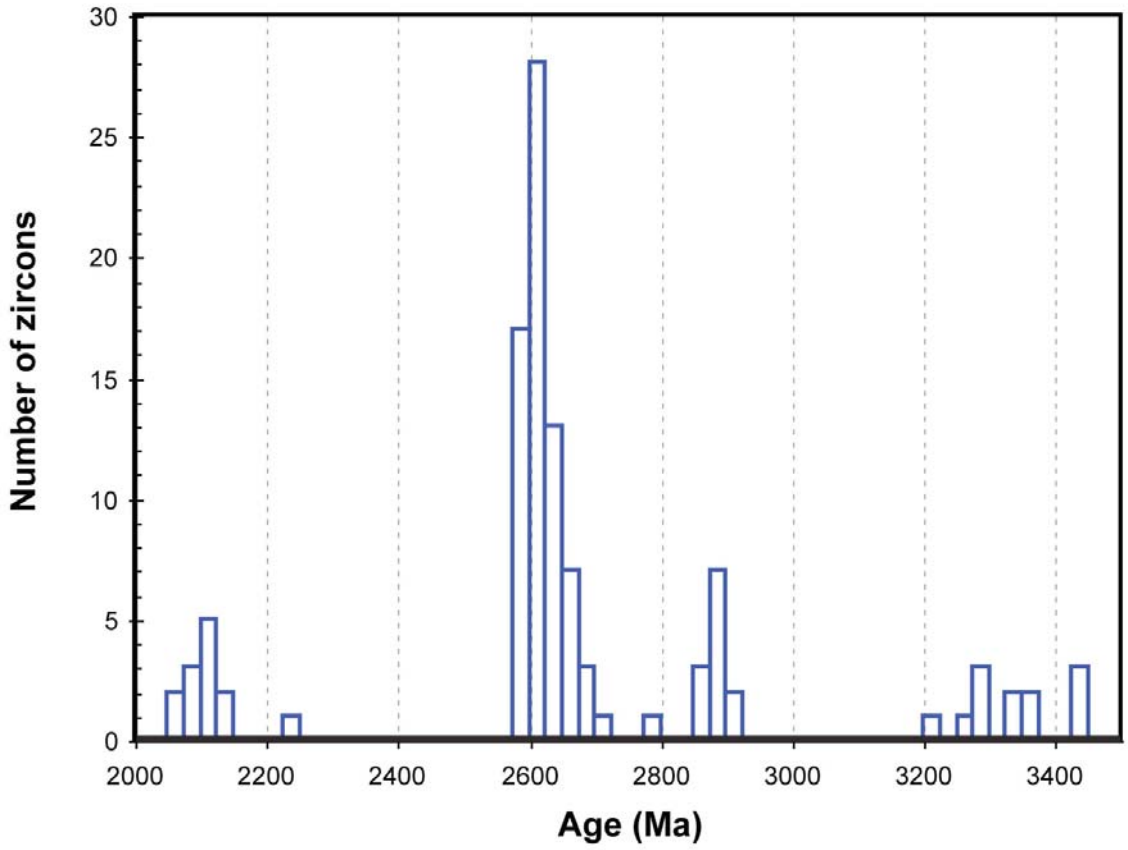

Figure 7: Frequency histogram of ages of zircons more than 90% concordant from sample 05KP30. The reported ages are $^{207}Pb/^{206}Pb$ ages. The groups of zircons around 2,100 Ma, 2,625 Ma, 2,900 Ma, 2,200 Ma and 2,450 Ma are apparent here.

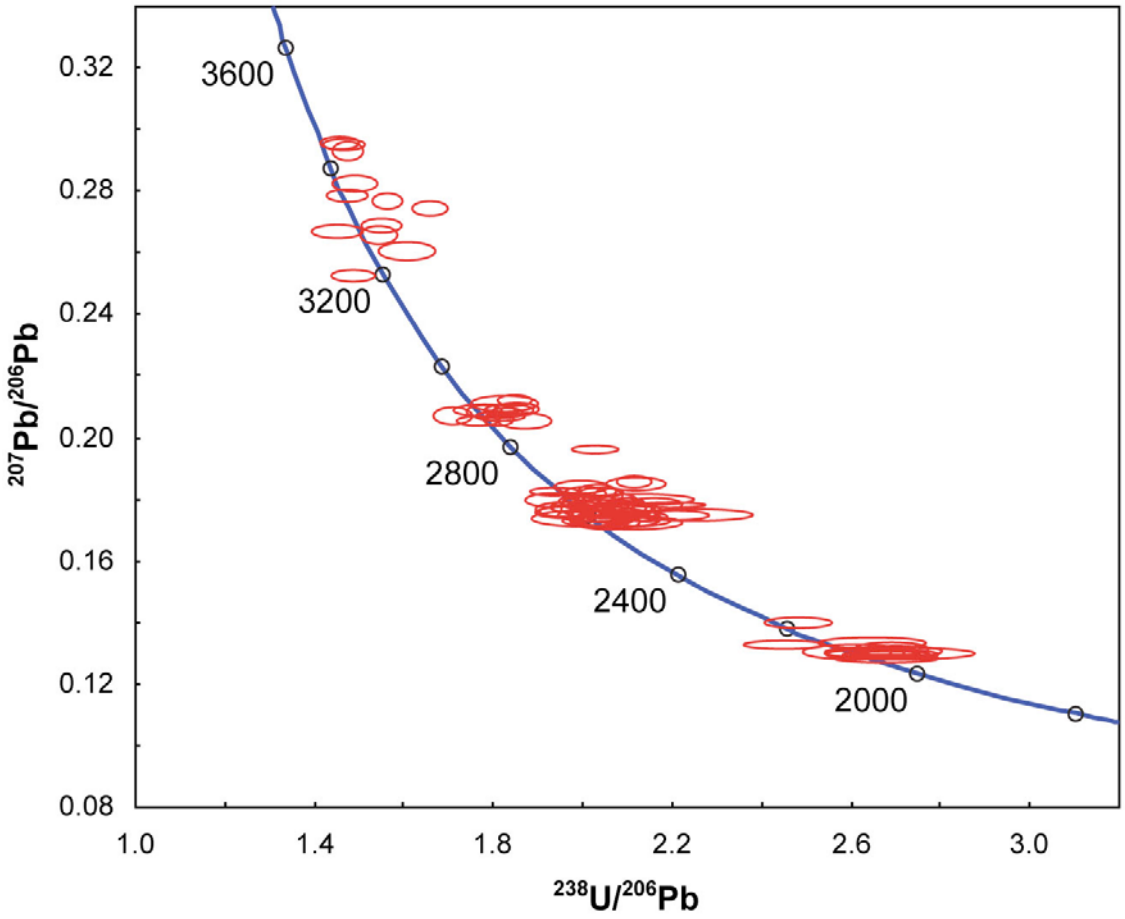

Figure 8: Inverse concordia diagram showing zircon ages from sample 05KP30 with error ellipses of 2σ. Only zircons that are more than 90% concordant are shown.

Sample 05KP32

Of the 106 grains (and 126 total analyses) from this sample, 54 are more than 90% concordant, 38 are less than 90% concordant, 27 can only be used for $^{207}Pb/^{206}Pb$ ages, and 7 were culled. A spreadsheet with all analyses and errors is included as appendix D. In this sample the concordant analyses are the focus, but the discordant analyses are also of interest to make the results more robust. Of the concordant samples, the youngest zircon grain is 2,173±11 Ma. The oldest grain is 3,505±8 Ma. Within that

range there two major spikes in age frequencies. One ranges from approximately 2,600 Ma to 2,800 Ma and another appears at approximately 3,400MGa. A histogram was made using only the analyses that are more than 90% concordant (figure 9). An inverse concordia diagram with only those zircons that are more than 90% concordant is also included (Figure 10), showing the clusters in ages with error ellipses of 2σ.

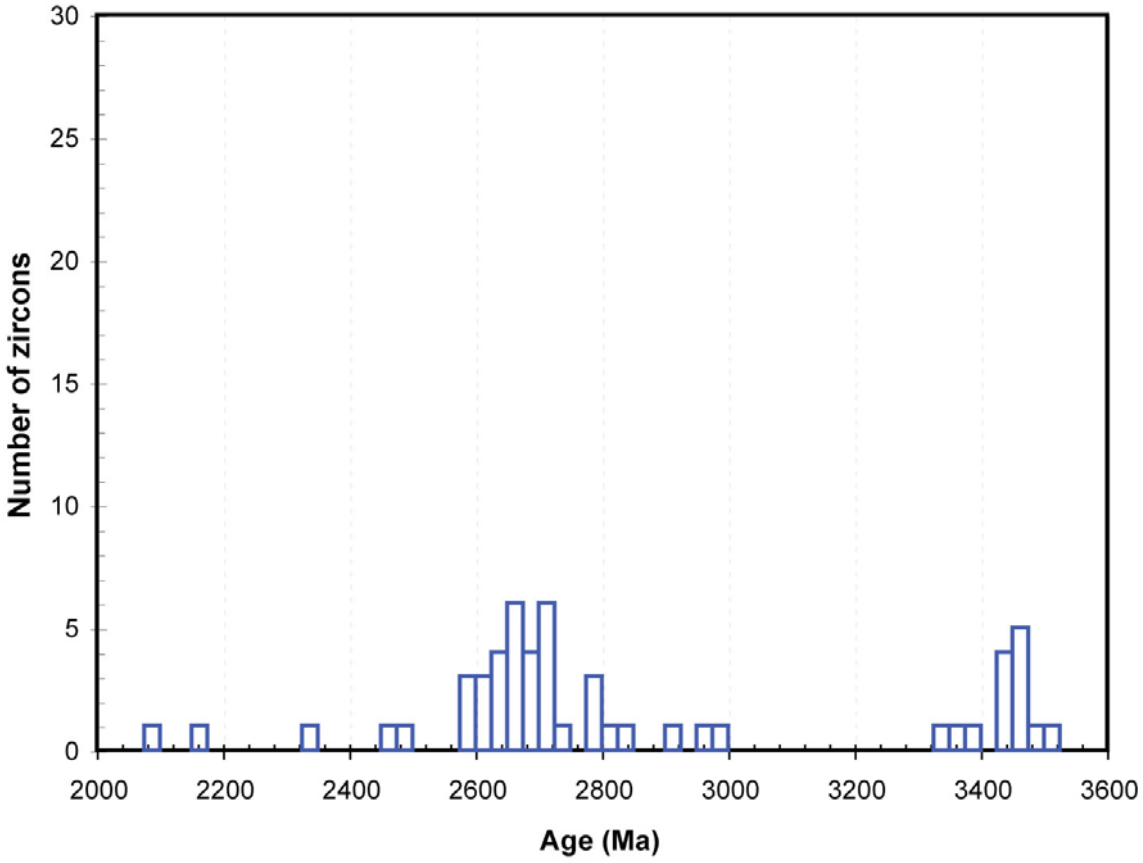

Figure 9: Frequency histogram analyses that are more than 90% concordant from sample 05KP32. The reported ages are $^{207}Pb/^{206}Pb$ ages. The major groups of zircons are apparent between 2,600 Ma and 2,800 Ma, and between 3,360 Ma and 3,500 Ma.

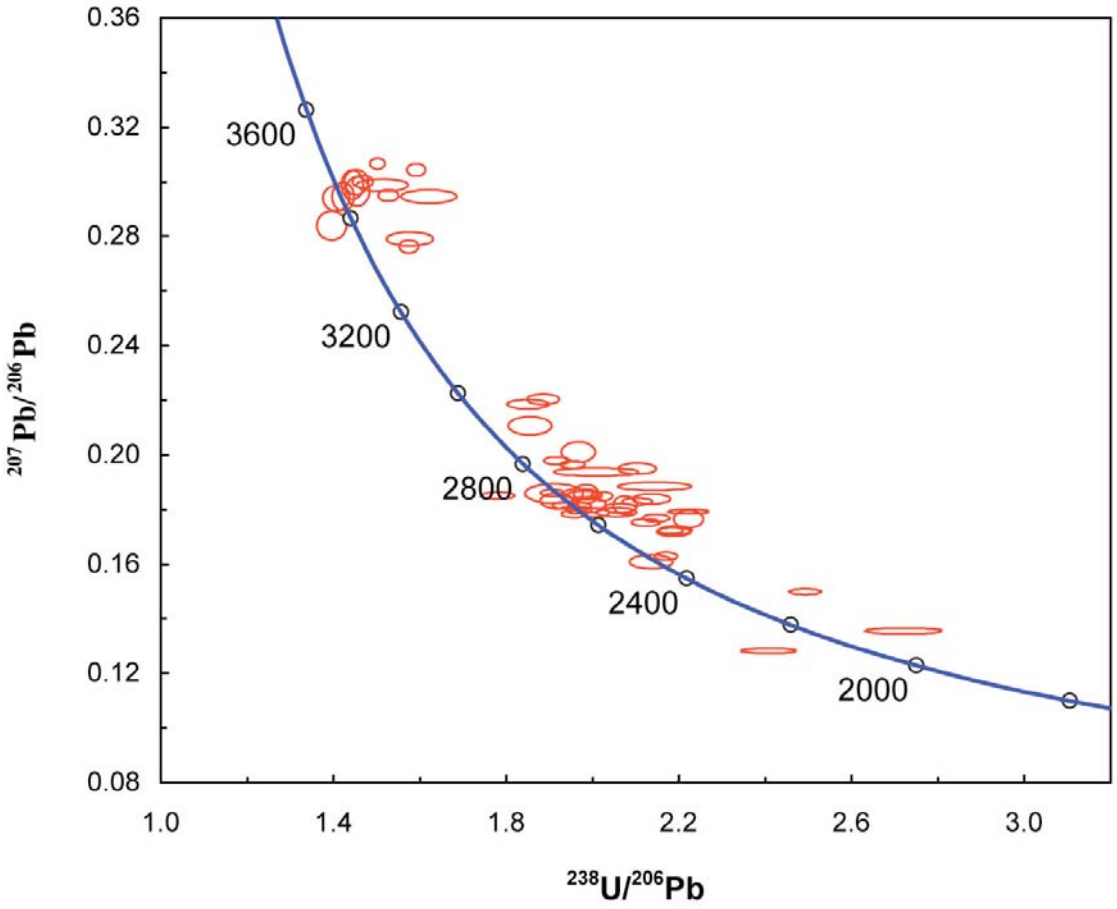

Figure 10: Inverse concordia diagram showing zircon ages from sample 05KP32 with error ellipses of 2σ. Only zircons that are more than 90% concordant are shown.

In some cases when all of the discordant zircons in a sample have similar morphologies or there is a pattern to the discordant ages, an assumption can be made about their actual age and about the age of the lead loss that made them discordant. This is not very accurate to do unless there is strong evidence that all of the zircons came from the same source. For example, if all of the zircons came from one granite and they are all discordant, a line called an isochron can be drawn through all the discordant points. The upper point where the isochron intersects the concordia line is the age of zircon

formation, and the lower point where the isochron intersects the concordia line is the age of lead loss. This can be used to find actual ages of zircons, even when they have been altered in some way, and to find the time that they were altered. In this case, however, there is no strong case from either the zircon morphologies or the concordia diagram showing that the zircons represent distinct populations. Figure 11 is a histogram showing the ages that are more than 90% concordant (blue), the ages that are less than 90% concordant (red) and the ages that can only be used for $^{207}Pb/^{206}Pb$ ages (green). On this histogram with all of the analyses represented, it is apparent that in many places the discordant grains and the $^{207}Pb/^{206}Pb$ only grains add frequency to the concordant grains instead of adding completely different ages.

Figure 12 is a concordia diagram that illustrates this including the zircons that are more than 90% concordant in blue and the ones that are less than 90% concordant in green. The discordant zircons are farther away from the concordia line so it is farther to project to find the age. Because of this the ages are more inaccurate so they are not included in the interpretations or in Figures 9 and 10.

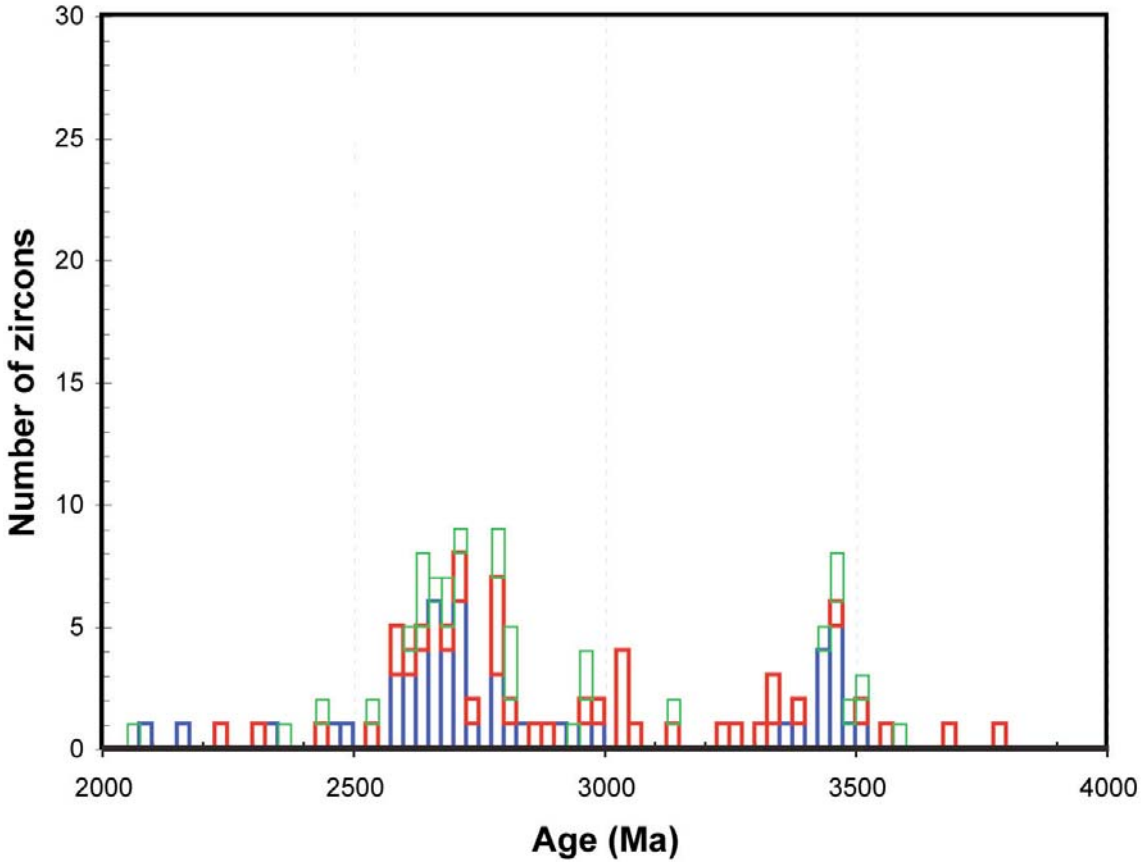

Figure 11: Frequency histogram of concordant (blue) discordant (red) and $^{207}Pb/^{206}Pb$ only (green) analyses from sample 05KP32. All reported ages are $^{207}Pb/^{206}Pb$. This shows that for the most part the discordant and $^{207}Pb/^{206}Pb$ ages are similar to the concordant ages and make the data more robust.

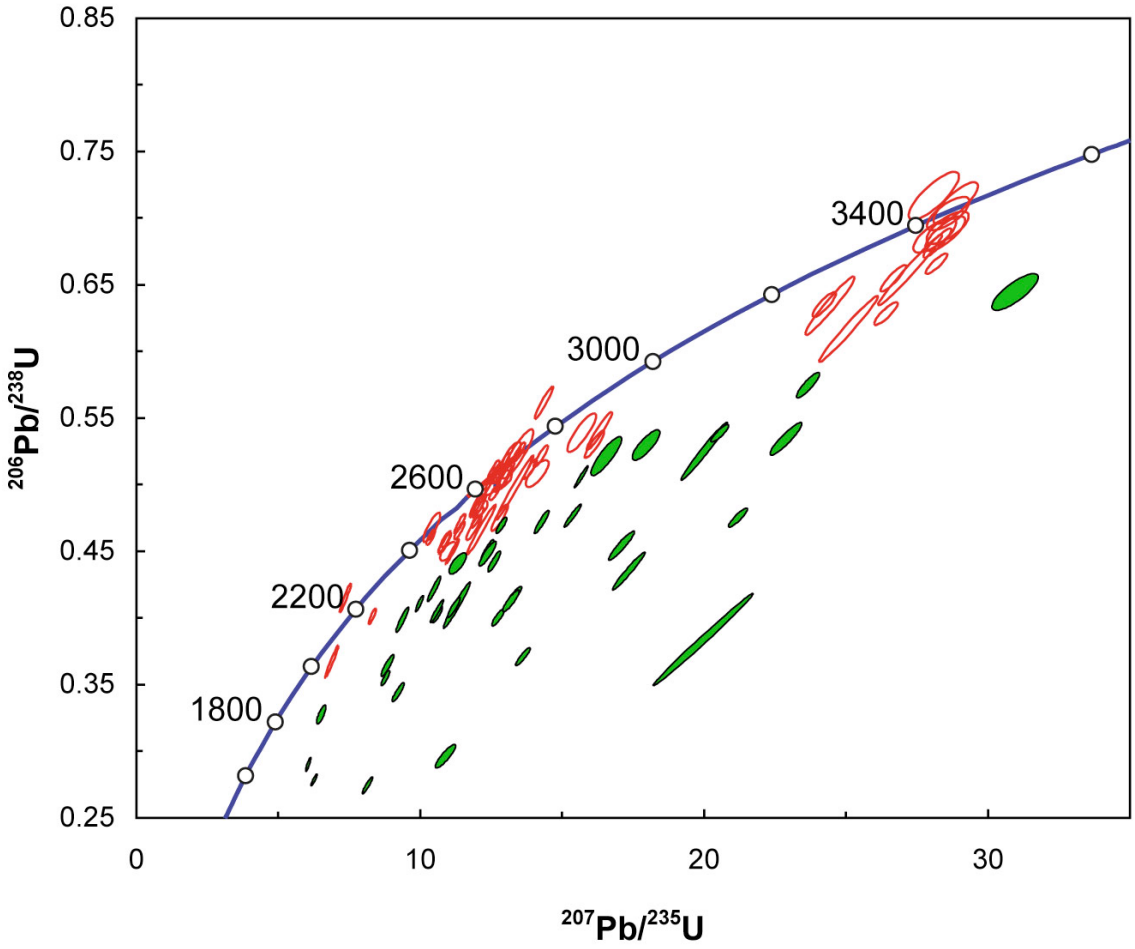

Figure 12: Concordia diagram including the analyses that are more than 90% concordant (red) and the analyses that are less than 90% concordant (green) from sample 05KP32. Error ellipses are 2σ. It is evident here that it would be difficult to place the discordant grains in distinct populations to analyze them.

Sample 05KP36

This sample yielded only one small grain on which two analyses could be done. Unfortunately, the fact that there was only one zircon recovered from the rocks is statistically problematic and the analyses are both more than 10% discordant. The

analyses and errors are compiled in appendix E. The ages are 1962±9 Ma and 1929±10 Ma. An inverse concordia diagram (Figure 13) shows the two results.

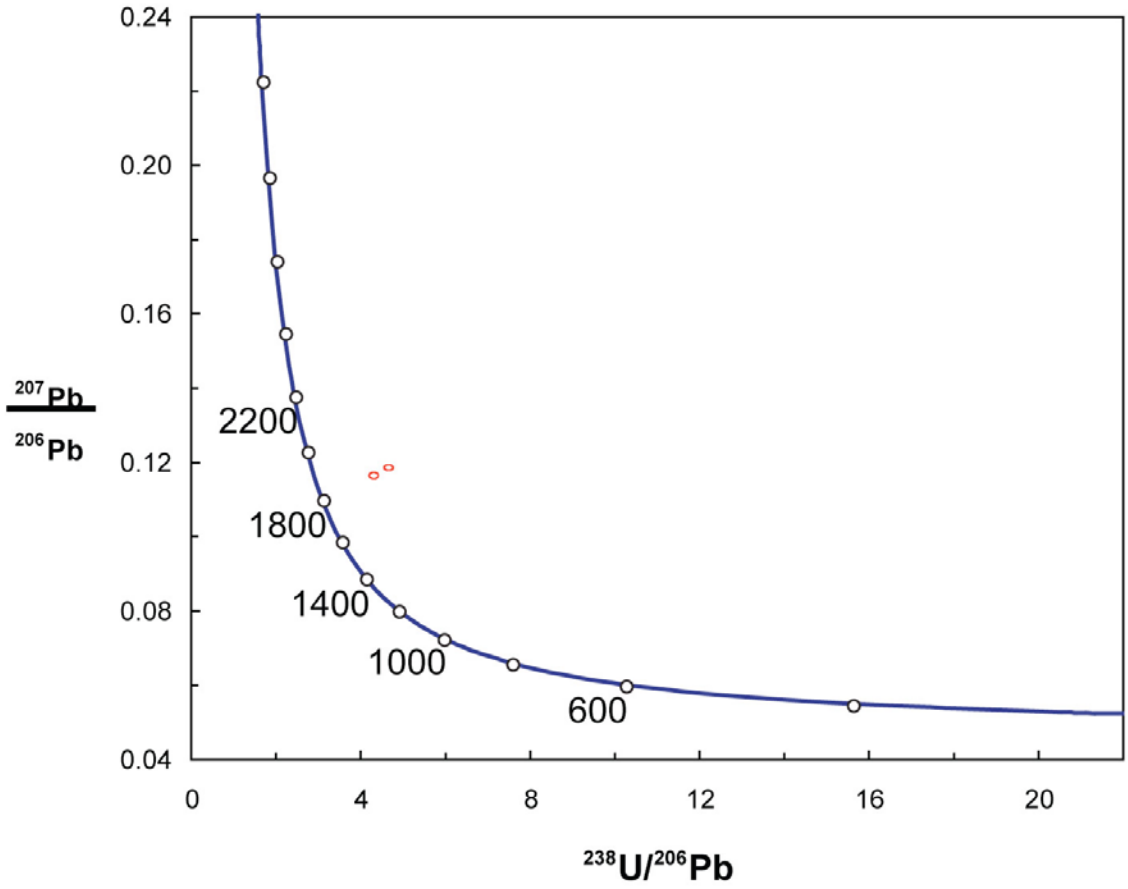

Figure 13: Inverse concordia diagram for the two results from the single zircon grain from sample 05KP36. The error ellipses are 2σ.

Whole rock geochemistry

The XRF data for the Denham meta-basalt are included as appendix F. The meta-basalt has normative plagioclase and orthoclase, diopside, olivine, and nepheline. It has 53% SiO_2 and 7% Na_2O+K_2O. This chemistry makes the basalt part of the alkaline series (Figure 14). A petrologic diagram is included. Figure 15 is a triangle plot of trace elements Y/15, La/10, and Nb/8 showing that, within measurement and graphical error,

the trace element composition may also indicate an alkaline composition. Figure 16 is a plot of V and Ti/1000 showing that, within error, those elements may also indicate an alkaline composition or a MORB.

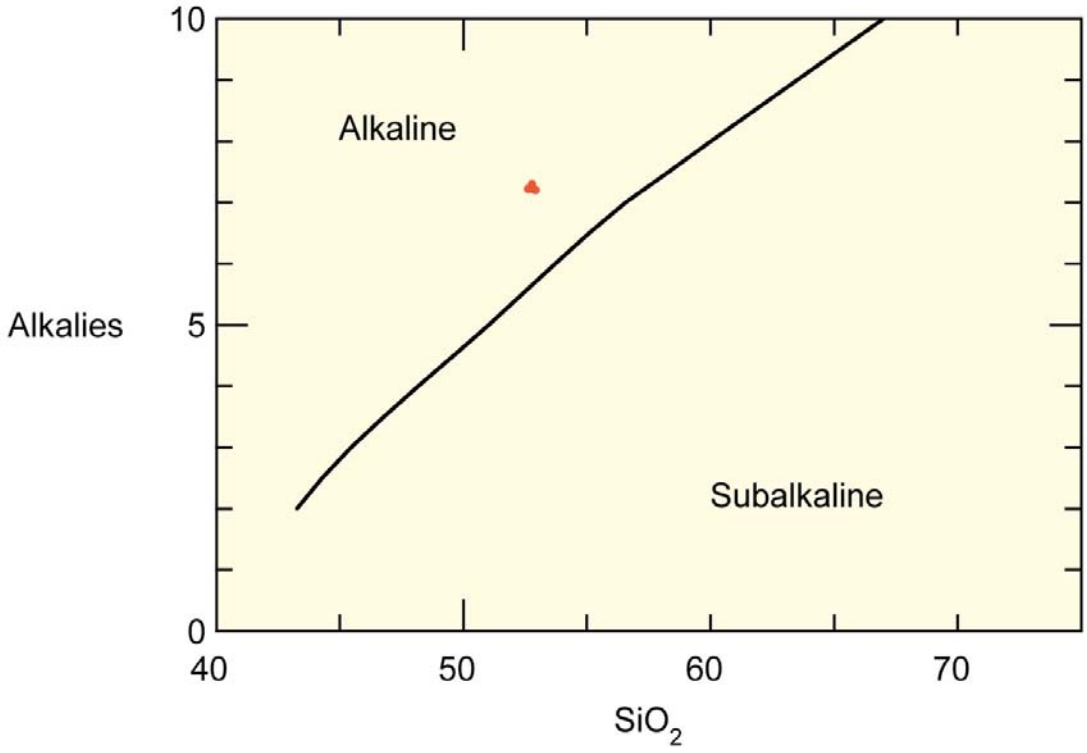

Figure 14: Plot of wt% SiO_2 versus alkalies in the Denham meta-basalt. This shows that, according to these oxides, the meta-basalt has an alkaline composition.

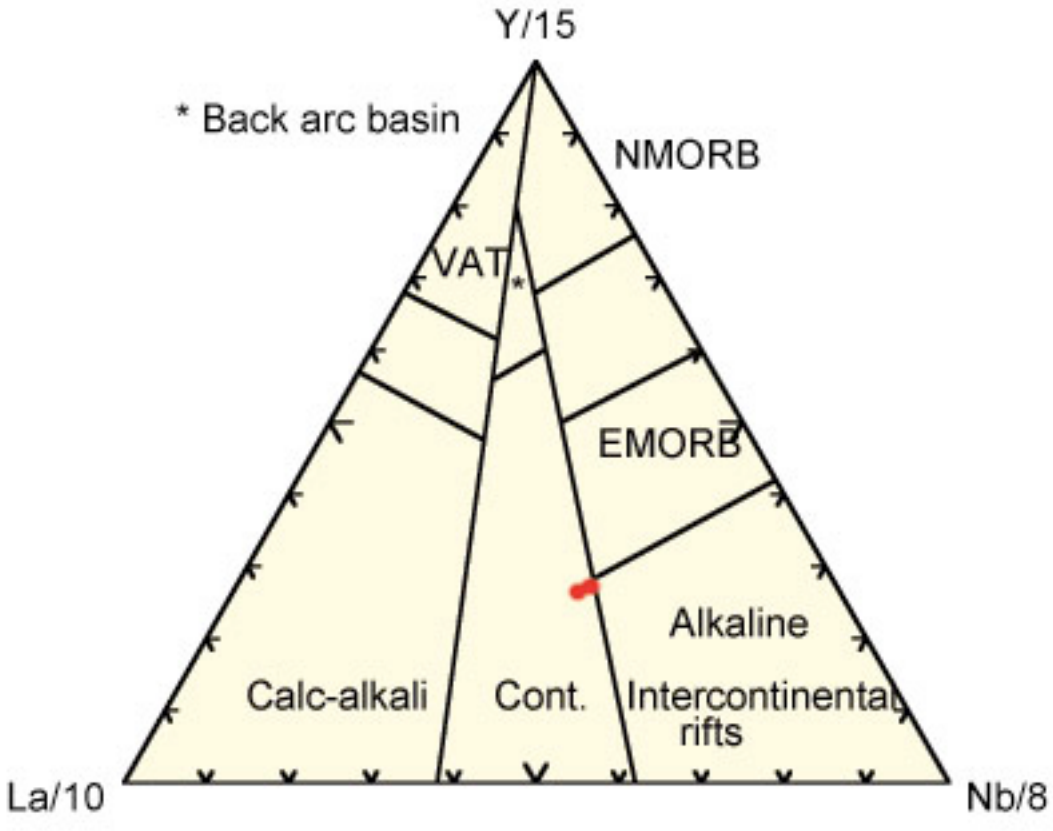

Figure 15: Plot of trace elements Y, La, and Nb in the Denham meta-basalt. The data (in red) fall on a line between EMORB, continental, and alkaline intercontinental rifts. This can be interpreted as being any of the three because of the uncertainty of exactly where the lines get drawn in these types of graphs.

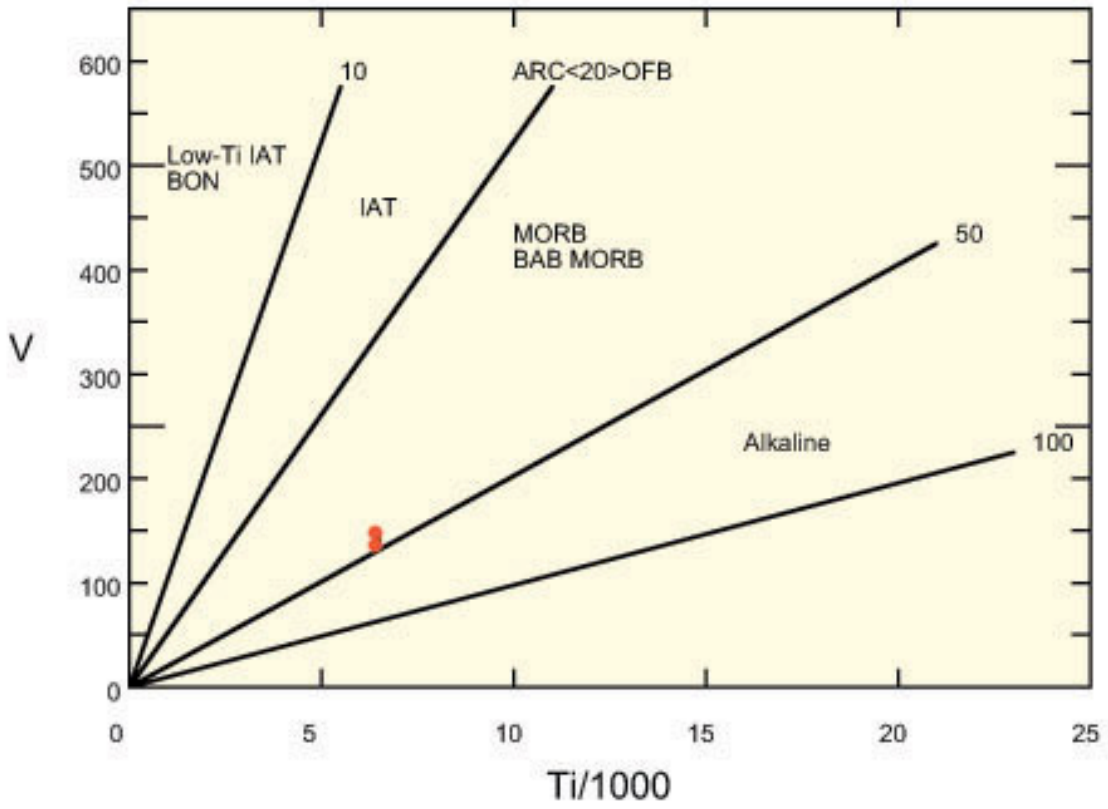

Figure 16: Plot of trace elements V and Ti in the Denham meta-basalt. The data (in red) fall on the line between an alkaline composition and a MORB composition. Once again this could indicate either one because of measurement and graphical errors.

Discussion

The whole rock chemistry of the Denham meta-basalt supports the hypothesis of the Denham area having been a continental rift margin at the end of the Kenorland breakup. Alkaline basalt is seen in different tectonic settings but is a common product of continental rifts, so the new evidence supports the proposed rift setting. One such continental rift that contains alkaline basalt is the East African Rift System. In the East African Rift the basalts start out as nephelenites and alkaline basalts and gradually turn into other compositions, taking on more MORB-like compositions, and eventually becoming silica-saturated (Blatt and Tracy, p. 198-202). This makes the rocks in the Denham formation likely to be from early to intermediate in the sequence of rifting, based upon the results (Figures 14-16) that place it as in between a MORB and alkaline composition. It is not known whether metabasalts of more evolved rift compositions exist, or whether the rift was aborted before such basalts were erupted. Whether the rift is initiated by a mantle plume or by some other extensional force (the latter is more likely in this case), the first magmas are mantle derived, probably in the upper asthenosphere. The first magma to melt moves up through the crust and lithosphere, thinned by the extensional force. This model is supported by the high concentrations of incompatible elements in the Denham meta-basalt.

The first conclusion that can be reached from the LA-ICPMS analyses is the age of the Denham formation. It must be older than the 2,009 Ma cross-cutting dikes (Holm et al., 2005) and younger than the youngest zircon found (2,073±18 Ma in sample 05KP30). It must be younger than the youngest zircon found because all of the sediment

would have been deposited along with the zircons and then it would have lithified. These ages place a tight constraint on the age of the Denham.

The source interpretations made are illustrated on a histogram (Figure 16) and a map of Minnesota (Figure 17). Not all of the zircons found have an interpretation for a source region because a lot of time has gone by and not every rock in the area has been dated. For these reasons some sources may no longer exist, have not been found yet, or they have not been dated correctly.

The ages from sample 05KP36 are most likely metamorphic. They seem to be older than the Penokean Orogeny, but that is still the most likely explanation for these ages.

The Morton and Montevideo Gneisses are most likely the sources for the zircons dated between 3,385 Ma and 3,500 Ma. In sample 05KP30 the zircons that are within this age group and more than 90% concordant are not very rounded or weathered looking. They have a somewhat euhedral shape and are subangular. This indicates that they did not travel in a high-energy environment to the Denham from the Minnesota River Valley. They are zoned, which is expected because they were formed in a granite where they would have grown slowly, and because of the many zircon forming events recorded in the Minnesota River Valley Gneisses.

Younger than the Morton and Montevideo Gneisses are the zircons probably originating in the far north of the Superior Province. These range between the ages of 3,200 Ma and 3,370 Ma. These zircons range from euhedral to subrounded. Many of them are zoned. The fact that they would have had to travel a long distance to come from central Canada to reach the Denham, but they are still euhedral and zoned, suggests that

these zircons may have been reworked into different sedimentary or igneous rocks before being deposited in the Denham basin.

There are zircons from both sample 05KP30 and 05KP32 that are between the ages of 2,963 Ma and 2,740 Ma that may have originated from the Wabigoon Greenstone Subprovince. If the Wabigoon Greenstones are in fact as young as 2,250 Ma, then the zircons between 2,300 Ma and 2,500 Ma may have originated there as well. It is possible that the large groupings of zircons between the ages of 2,575 Ma and 2,601 Ma are from both the Sacred Heart Granite and the Benson Block Granite from the Minnesota River Valley. This possibility is supported by the presence of two distinct zircon morphologies in the sample. Of the more than 90% concordant zircons that are between 2,575 Ma and 2,601 Ma in samples 05KP30 and 05KP32 some of them are distinctly zoned and euhedral while others are rounded and the zoning is cut off by the weathering of the grains. It is uncertain which population came from which source, as they are approximately the same distance away from the Denham.

Zircons between the ages of 2,650 Ma and 2,750 Ma may have originated in rocks created by the Kenoran Orogeny. These are mostly intrusive igneous rocks in northern Minnesota. This time period overlaps with the time frame for the Wawa Greenstone Subprovince, so the zircons could have come from just the Kenoran Orogeny rocks or from both.

Hemming et al. (1995) suggest that ages around 2,100 Ma and 2,200 Ma in younger rocks can possibly be attributed to Proterozoic rocks that we have no current record of. This may also be the case for these ages in the Denham formation.

In neither sample 05KP30 nor sample 05KP32 is there a pattern of ages or morphologies of discordant zircons. No interpretation of their source region or of their age of lead loss was made.

There are few concordant zircons with ages near the 2,557 Ma age of the McGrath gneiss. This is a very surprising result that this closest obvious source of zircons for the Denham rocks does not have definitive representation in the zircon age distribution. Instead of the hypothesis that the McGrath Gneiss eroded into an opening basin there must have been some other scenario where the McGrath did not provide sediment to the Denham formation and surrounding rocks contributed instead. The original rift theory assumed that the McGrath was in a position to be weathered and transported, which would mean that it had high relief and that there was a way for the sediment to get into the Denham rift. With the results from this study, this is disproved and instead another possibility is proposed. If the McGrath was down in the rift valley and having low relief, instead of on the side of or above the rift valley being eroded, there would have been little sediment derived from it, which is the case. The other possibility is that the transport mechanisms were not carrying sediment from the McGrath toward the Denham to be deposited.

The two main source regions, the greenstone subprovinces to the north and the Minnesota River Valley gneisses to the southeast (Figure 17) provide information about the flow of sediment in the Paleoproterozoic eon. Two main possibilities exist for this occurrence. Either there were two separate transportation mechanisms, most likely streams, that flowed into the Denham rift valley separately, or there were two stream systems that met somewhere in the middle and flowed into the Denham area together.

The way to answer this question would be to examine Paleoproterozoic sedimentary rocks in other areas of the state and determine which areas had contributions from one source area or the other and analyze the stream systems that way.

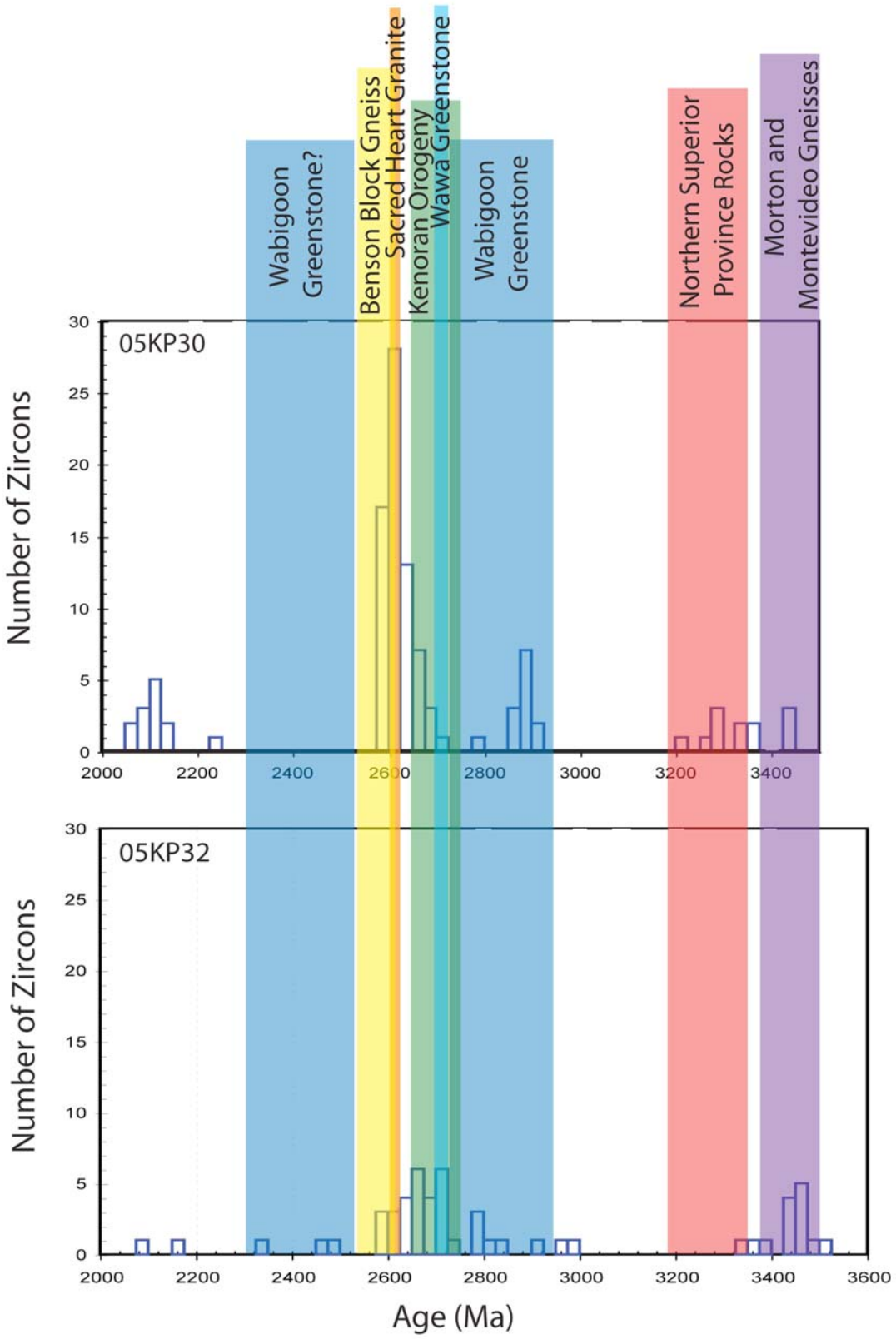
Wabigoon Greenstone?
Benson Block Gneiss
Sacred Heart Granite
Kenoran Orogeny
Wawa Greenstone
Wabigoon Greenstone
Northern Superior Province Rocks
Morton and Montevideo Gneisses
05KP30
05KP32
Number of Zircons
Age (Ma)

Figure 17: Histograms of samples 05KP30 and 05KP32 showing zircons that are more than 90% concordant. The different colored boxes indicate the age ranges of the potential source areas of the zircons.

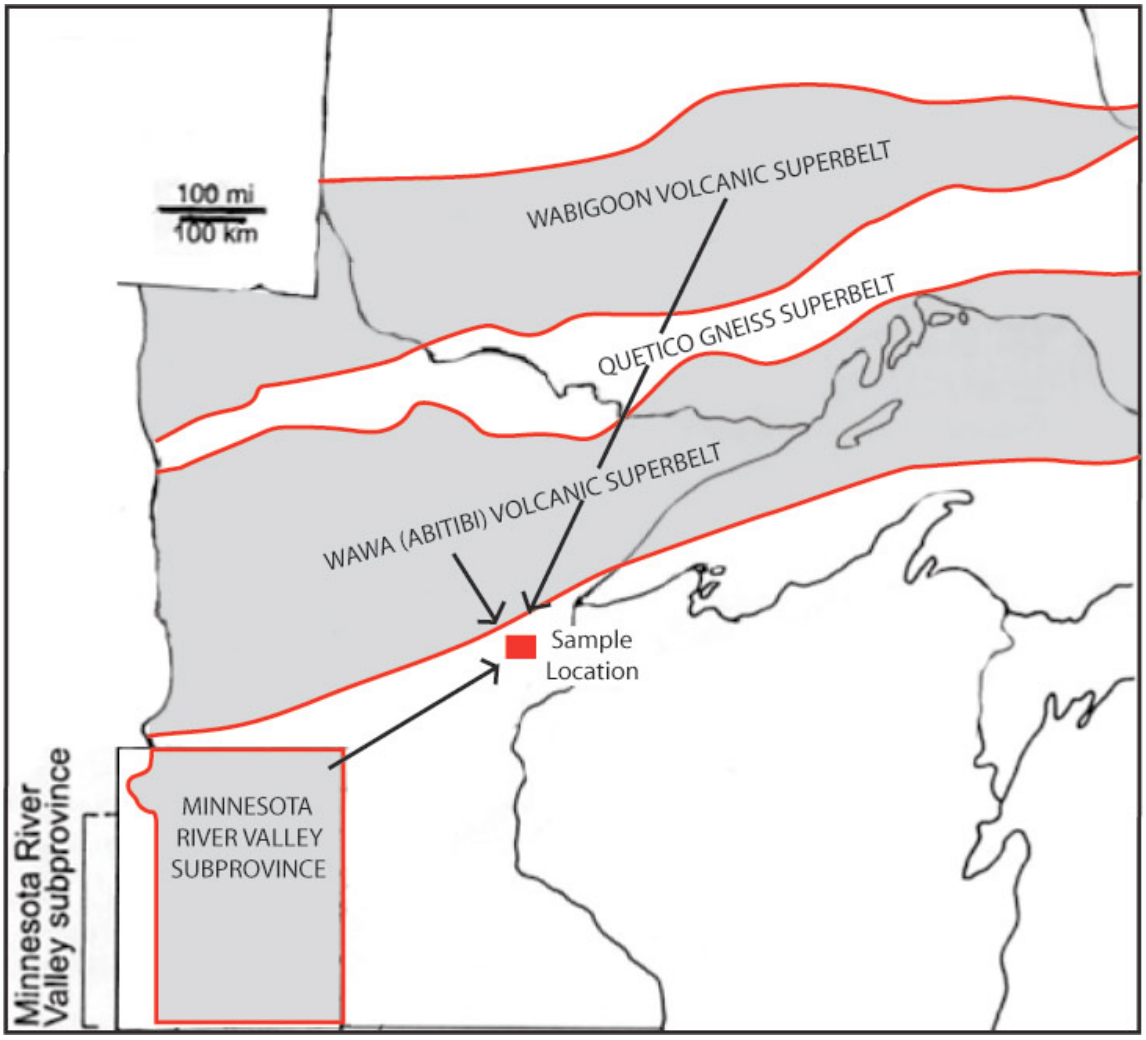

Figure 18: Simplified map of Minnesota showing source region locations in relation to the Denham Formation. Study area in the red box (data from Ojakangas and Matsch, 1982 p. 26 and Schmitz et al., 2006)

Conclusions

The main goals of this study, determining the tectonic setting and the source regions for the sediment, were accomplished. The conclusions reached are as follows:

1) Whole-rock geochemistry of the meta-basalt in the middle of the Denham section shows an alkaline composition. It has normative plagioclase, orthoclase, diopside, olivine, and nepheline. It has 53% SiO_2 and 7% Na_2O+K_2O. An alkaline composition is common in continental rifts, so the geochemical data support a rift theory.
2) The lowest conglomeratic arkose in the sequence has four major groupings of ages at around 2,100 Ma, 2,625 Ma, 2,900 Ma, 3,300 Ma and 3,450 Ma. The youngest zircon grain is 2,072±17 Ma and the oldest grain is 3447±17 Ma.
3) In the middle of the sequence is a dolomitic arkose that has major age groupings are between 2,600 Ma and 2,800 Ma, and between 3,360 Ma and 3,500 Ma. The youngest zircon grain is 2,173±11 Ma and the oldest grain is 3,505±8 Ma.
4) The age of the Denham can also be constrained by the results. It must be older than the 2,009 Ma cross-cutting dikes (Holm et al., 2005) and younger than the youngest zircon found (2,073±18 Ma in the lowest sample).
5) Sediment in the Denham Formation originated in the Minnesota River Valley Subprovince to the southeast, the Greenstone Subprovinces to the north, the rocks created by the Kenoran Orogeny to the north and rocks in the northern part of the Superior Province in Canada.

References

Andersen, T., 2005, Detrital zircons as tracers of sedimentary provenance; limiting conditions from statistics and numerical simulation: Chemical Geology, v. 216, p.249-270.

Aspler, L.B., 2001, Paleoproterozoic intracratonic basin processes, from breakup of Kenorland to assembly of Laurentia: Hurwitz Basin, Nunavut, Canada: Sedimentary Geology, v. 141-142, p. 287-318.

Beck, J.W., 1988, Implications for early Proterozoic tectonics and the origin of continental flood basalts, based on combined trace element and neodymium/strontium isotopic studies of mafic igneous rocks of the Penokean Late Superior belt, Minnesota, Wisconsin, and Michigan: Minneapolis, University of Minnesota, Ph.D. dissertation, 273 p.

Bickford et al., 2006, SHRIMP study of zircons from early Archean rocks in the Minnesota River valley; implications for the tectonic history of the Superior Province, Bickford: Geological Society of America Bulletin, v. 118, p. 94-108.

Blatt, H., and Tracy, R., 1996, Petrology, 2nd ed.: W.H. Freeman and Company.

Boerboom, T.J., Jirsa, M.A., 2001, Stratigraphy of the Paleoproterozoic Denham Formation; a continental margin assemblage of basalt, arkose, and dolomite, *in* Proceedings and Abstracts, Institute on Lake Superior Geology, v. 47, part 1, p. 6-7.

Boggs, S., 2001, Principles of sedimentology and stratigraphy, 3rd ed.: Upper Saddle River, N.J., Prentice Hall.

Chang, Z., Vervoort, J.D., McClelland, W.C., and Knaack, C., 2006, U-Pb dating of zircon by LA-ICP-MS, submitted.

Ermanovics, I.F., and Wanless, R.K., 1983, Isotopic age studies and tectonic interpretation of Superior Province in Manitoba: Paper-Geological Survey of Canada, v. 82-12, p. 1-22.

Faure, G., 1998, Principles and applications of geochemistry, 2nd ed.: Upper Saddle River, N.J., Prentice Hall.

Feng, R., Machado, N., and Ludden, J., 1993, Lead geochronology of zircon by laser probe–inductively coupled plasma mass spectrometry (LP–ICPMS): Geochimica et Cosmochimica Acta, v. 57, p. 3479–3486.

Fryer, B.J., Jackson, S.E., and Longerich, H.P., 1993, The application of laser ablation microprobe–inductively coupled plasma mass spectrometry (LAM–ICPMS) to in situ (U)–Pb geochronology: Chemical Geology, v. 109 , p. 1–8.

Hemming, S.R., 1995, Geochemical and Nd/Pb isotopic evidence for the provenance of the early Proterozoic Virginia Formation, Minnesota: implications for the tectonic setting of the Animikie Basin: Journal of Geology, v. 103, p. 147-168.

Holm, D.K., Van Schmus, W.R., MacNiell, L.C., Boerboom, T.J., Schweitzer, D., and Schneider, D., 2005, U-Pb zircon geochronology of Paleoproterozoic plutons from the northern mid-continent, USA: Evidence for subduction flip and continued convergence after geon 18 Penokean orogenesis: Geological Society of America Bulletin, v. 117, p. 259-275.

Kosler, J., 2002, U-Pb dating of detrital zircons for sediment provenance studies; a comparison of laser ablation ICPMS and SIMS techniques: Chemical Geology, v. 182, p.605-618.

McKenzie, M.A., 2004, Age pattern and nature of Late Paleoproterozoic metamorphism of the Penokean crust, east-central Minnesota [M.S. thesis]: Kent, Ohio, Kent State University, 105 p.

Ojakangas, R.W., Matsch, C.L., 1982, Minnesota's Geology: Minneapolis, University of Minnesota Press.

Prothero, D.R., Schwab, F., 2004, Sedimentary Geology, 2nd ed.: New York, W. H. Freeman and Company.

Schmitz et al., 2006, High-precision U-Pb geochronology in the Minnesota River Valley Subprovince and its bearing on the Neoarchean to Paleoproterozoic evolution of the southern Superior Province: Geological Society of America Bulletin, v. 118, p.82-93.

Sircombe, Keith N., 2002, An investigation of artificial biasing in detrital zircon U-Pb geochronology due to magnetic separation in sample preparation, Sircombe, Keith N.: Geochimica et Cosmochimica Acta, v. 66, p. 2379-2397.

Thurston, P.C., 2002, Tectonic Controls on Mafic Magmatism in the Superior Province, *in* Abstract with Programs, International Platinum Symposium, 9th, p. 445-448.

Tomlinson, K., Condie, K., 2001, Archean mantle plumes: Evidence from greenstone belt geochemistry: Geological Society of America Special Paper 352, p.341-357.

Windley, B.F., 1995, The Evolving Continents, 3rd ed.: W. Sussex, England: John Wiley and Sons, Ltd.

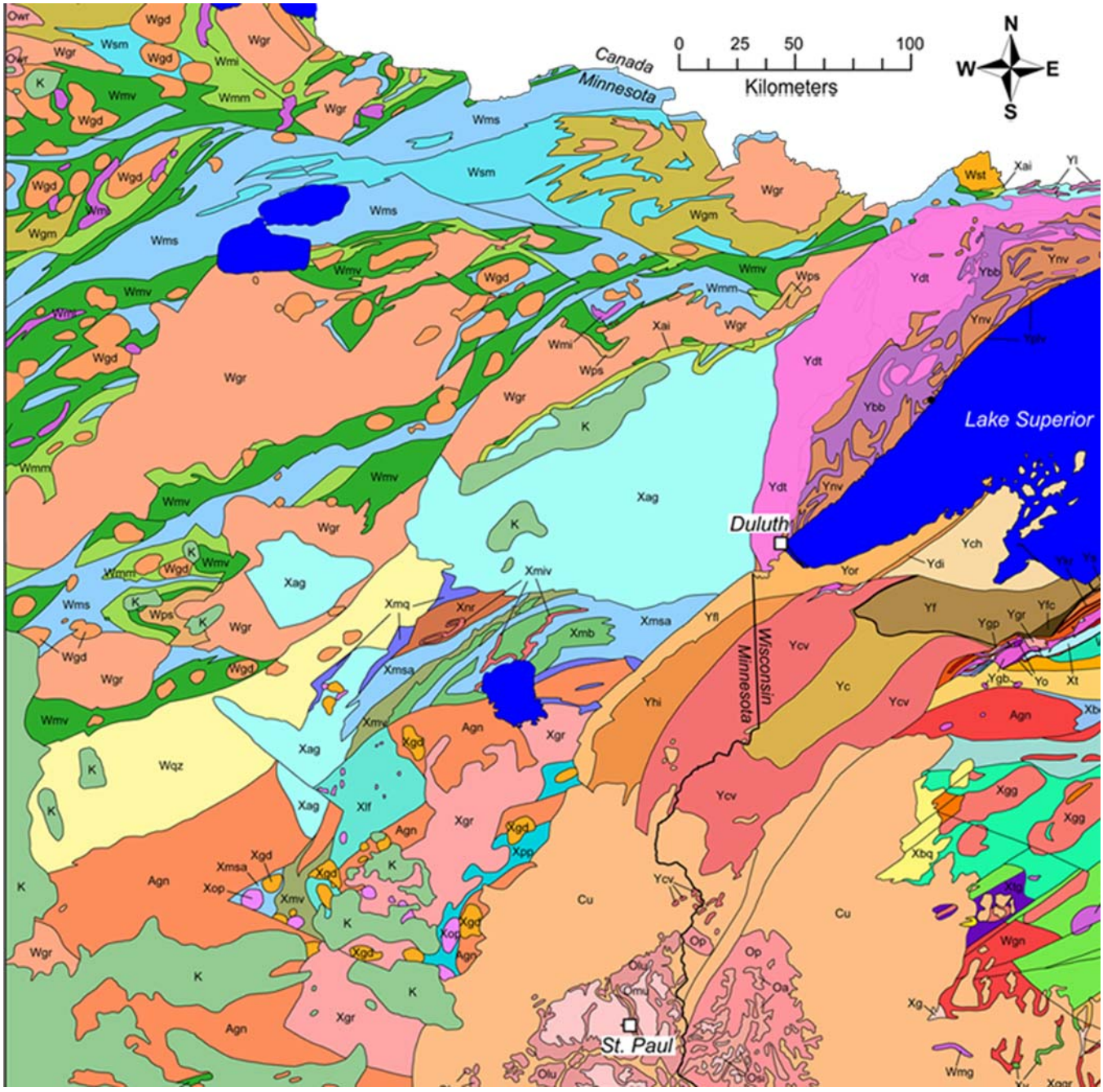
Canada
Minnesota
0 25 50 100
Kilometers
N
W
E
S
Lake Superior
Duluth
St. Paul
Wisconsin
Minnesota

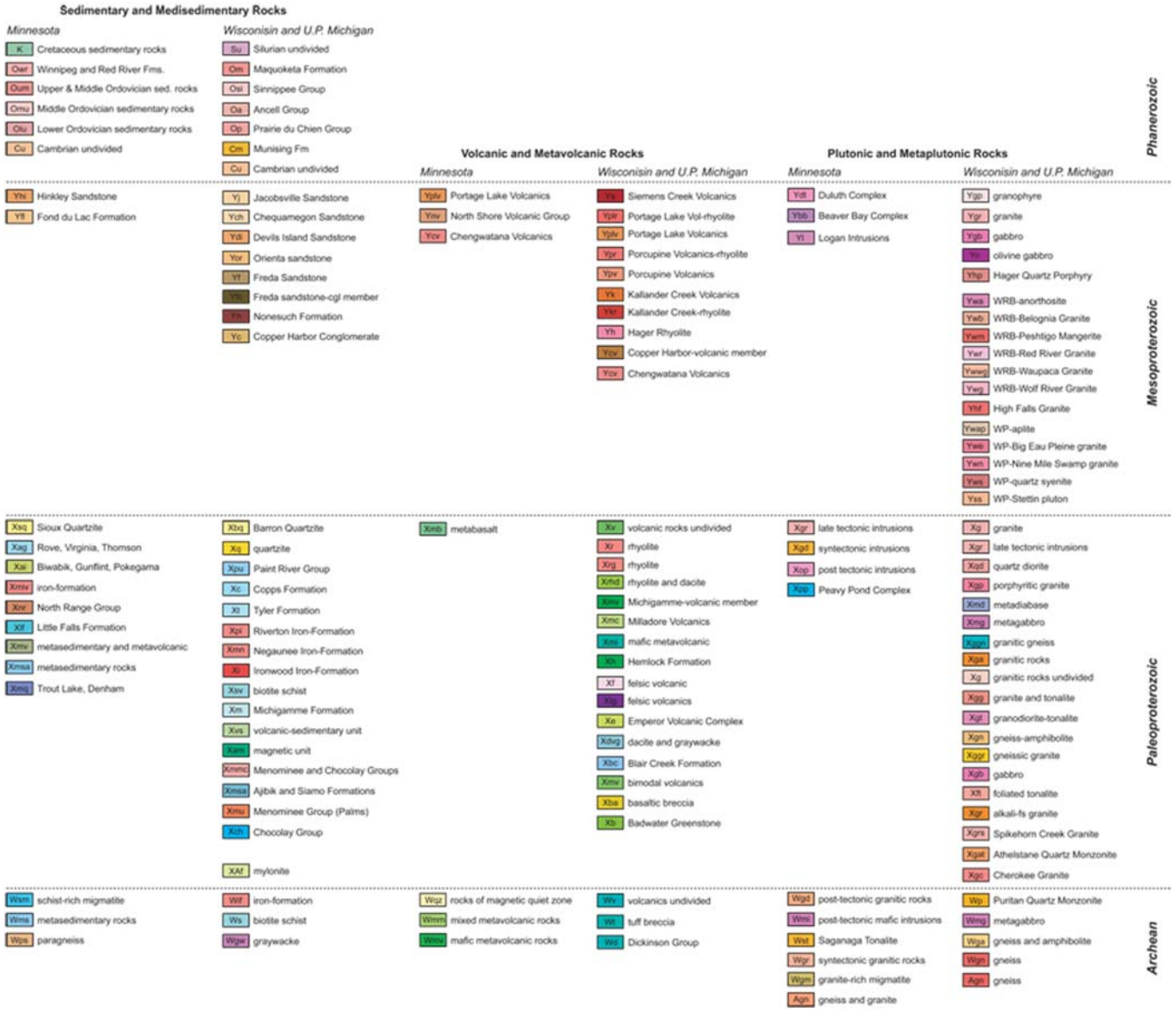
Sedimentary and Medisedimentary Rocks
Minnesota
K Cretaceous sedimentary rocks
Owr Winnipeg and Red River Fms.
Oum Upper & Middle Ordovician sed. rocks
Omu Middle Ordovician sedimentary rocks
Olu Lower Ordovician sedimentary rocks
Cu Cambrian undivided
Wisconisin and U.P. Michigan
Su Silurian undivided
Om Maquoketa Formation
Osi Sinnippee Group
Oa Ancell Group
Op Prairie du Chien Group
Cm Munising Fm
Cu Cambrian undivided
Yhi Hinkley Sandstone
Yfl Fond du Lac Formation
Yj Jacobsville Sandstone
Ych Chequamegon Sandstone
Ydi Devils Island Sandstone
Yor Orienta sandstone
Yfl Freda Sandstone
Yfsc Freda sandstone-cgl member
Yno Nonesuch Formation
Yc Copper Harbor Conglomerate
Volcanic and Metavolcanic Rocks
Minnesota
Yplv Portage Lake Volcanics
Ynv North Shore Volcanic Group
Ycv Chengwatana Volcanics
Wisconisin and U.P. Michigan
Ysi Siemens Creek Volcanics
Yplr Portage Lake Vol-rhyolite
Yplv Portage Lake Volcanics
Ypr Porcupine Volcanics-rhyolite
Ypv Porcupine Volcanics
Yk Kallander Creek Volcanics
Ykr Kallander Creek-rhyolite
Yh Hager Rhyolite
Ycv Copper Harbor-volcanic member
Ycv Chengwatana Volcanics
Plutonic and Metaplutonic Rocks
Minnesota
Ydl Duluth Complex
Ybb Beaver Bay Complex
Yl Logan Intrusions
Wisconsin and U.P. Michigan
Ygp granophyre
Ygr granite
Ygb gabbro
Yo olivine gabbro
Yhp Hager Quartz Porphyry
Ywa WRB-anorthosite
Ywb WRB-Belognia Granite
Ywm WRB-Peshtigo Mangerite
Ywr WRB-Red River Granite
Ywwg WRB-Waupaca Granite
Ywg WRB-Wolf River Granite
Yhf High Falls Granite
Ywap WP-aplite
Ywe WP-Big Eau Pleine granite
Ywn WP-Nine Mile Swamp granite
Yws WP-quartz syenite
Yss WP-Stettin pluton
Phanerozoic
Mesoproterozoic
Paleoproterozoic
Archean
Xsq Sioux Quartzite
Xwg Rove, Virginia, Thomson
Xw Biwabik, Gunflint, Pokegama
Xmiv iron-formation
Xnr North Range Group
Xlf Little Falls Formation
Xmsv metasedimentary and metavolcanic
Xmsa metasedimentary rocks
Xmtj Trout Lake, Denham
Xbq Barron Quartzite
Xq quartzite
Xpu Paint River Group
Xc Copps Formation
Xt Tyler Formation
Xpx Riverton Iron-Formation
Xmn Negaunee Iron-Formation
Xi Ironwood Iron-Formation
Xsv biotite schist
Xm Michigamme Formation
Xvs volcanic-sedimentary unit
Xam magnetic unit
Xmmc Menominee and Chocolay Groups
Xmsa Ajibik and Siamo Formations
Xmu Menominee Group (Palms)
Xch Chocolay Group
XAf mylonite
Xmb metabasalt
Xv volcanic rocks undivided
Xr rhyolite
Xrg rhyolite
Xrhd rhyolite and dacite
Xmv Michigamme-volcanic member
Xmc Milladore Volcanics
Xms mafic metavolcanic
Xh Hemlock Formation
Xf felsic volcanic
Xfg felsic volcanics
Xe Emperor Volcanic Complex
Xdvg dacite and graywacke
Xbc Blair Creek Formation
Xmv bimodal volcanics
Xba basaltic breccia
Xb Badwater Greenstone
Xgr late tectonic intrusions
Xgd syntectonic intrusions
Xop post tectonic intrusions
Xpb Peavy Pond Complex
Xg granite
Xgr late tectonic intrusions
Xqd quartz diorite
Xpp porphyritic granite
Xmd metadiabase
Xmg metagabbro
Xggn granitic gneiss
Xga granitic rocks
Xg granitic rocks undivided
Xgg granite and tonalite
Xgt granodiorite-tonalite
Xgn gneiss-amphibolite
Xggr gneissic granite
Xgb gabbro
Xft foliated tonalite
Xgr alkali-fs granite
Xgrs Spikehorn Creek Granite
Xgat Athelstane Quartz Monzonite
Xgc Cherokee Granite
Wsm schist-rich migmatite
Wms metasedimentary rocks
Wps paragneiss
Wif iron-formation
Ws biotite schist
Wgw graywacke
Wgz rocks of magnetic quiet zone
Wmm mixed metavolcanic rocks
Wmb mafic metavolcanic rocks
Wv volcanics undivided
Wtf tuff breccia
Wd Dickinson Group
Wgd post-tectonic granitic rocks
Wmi post-tectonic mafic intrusions
Wst Saganaga Tonalite
Wgr syntectonic granitic rocks
Wgm granite-rich migmatite
Agn gneiss and granite
Wp Puritan Quartz Monzonite
Wmg metagabbro
Wga gneiss and amphibolite
Wgn gneiss
Agn gneiss

Appendix B: Sample descriptions

Sample	Formation	Description and mineralogy	Bedding	Foliation	Lineation	UTM zone 17
KP05–30	McGrath Gneiss	Strong lineation and foliation. Quartz, feldspar, muscovite.		(256, 28)	(06, 270)	0503862 E 5132132 N
KP05–30c	Denham lower meta-arkose	Visible layering. Not very deformed. Beds range from pebble sized clast conglomerate to medium sand size. Quartz, biotite, muscovite, albite, microcline	(105, 70)		(11, 285)	0503862 E 5132132 N
KP05–31	Denham schist	Schistose texture with foliation and intersection lineation. Quartz, biotite, muscovite, calcite, microcline		(283, 48)	(04, 093)	0505416 E 5132373 N
KP05–32	Denham meta-conglomerate	Conglomeratic meta-sandstone. Quartz, biotite, muscovite, calcite, microcline	(297, 56)			0505375 E 5132482 N
KP05–33	Denham meta-basalt	Amphibolite has pillows and foliation. Quartz, hornblende, calcite, plagioclase		(273, 55)	(103, 06)	0505331 E 5132578 N
KP05–34	Denham meta-carbonate	Calcite, muscovite, quartz		(097, 78)	(095, 04)	0505383 E 5132772 N
KP05–35	Denham meta-dolomite	Calcite, muscovite, quartz		(315, 36)		0505192 E 5133128 N
KP05–36	Little Falls schist	Schistose texture. Has boudinaged quartz veins. Quartz, garnet, staurolite, biotite, muscovite, chlorite		(245, 90)	(245, 12)	0506378 E 5134247 N

Appendix C: Sample 05KP30

< 10% discordant

Sample #	$^{207}Pb/^{235}U$ intercept	2σ	$^{206}Pb/^{238}U$ intercept	2σ	$^{207}Pb/^{206}Pb$ average	2σ	$^{207}Pb/^{235}U$ age (Ma)	2σ	$^{206}Pb/^{238}U$ age (Ma)	2σ	$^{207}Pb/^{206}Pb$ age (Ma)	2σ	% discordant
05KP30_001a	6.7231	0.2139	0.3711	0.0099	0.1314	0.0013	2075.7	27.7	2034.6	46.2	2116.7	17.1	3.9%
05KP30_002a	12.0684	0.2704	0.4724	0.0079	0.1853	0.0014	2609.7	20.8	2494.1	34.7	2700.7	12.4	7.6%
05KP30_003a	11.8303	0.3160	0.4810	0.0106	0.1784	0.0014	2591.1	24.7	2531.7	46.0	2637.7	12.8	4.0%
05KP30_005a	11.3083	0.2792	0.4601	0.0091	0.1783	0.0013	2548.9	22.8	2439.9	40.0	2636.7	12.4	7.5%
05KP30_007a	15.7133	0.4635	0.5460	0.0137	0.2087	0.0017	2859.5	27.8	2808.5	56.9	2895.6	13.0	3.0%
05KP30_008a	12.2181	0.3040	0.4900	0.0098	0.1808	0.0014	2621.3	23.1	2570.6	42.1	2660.6	12.6	3.4%
05KP30_010a	15.9163	0.6051	0.5479	0.0186	0.2107	0.0020	2871.8	35.7	2816.5	77.0	2910.8	15.2	3.2%
05KP30_011a	11.6639	0.2426	0.4822	0.0092	0.1754	0.0008	2577.8	19.3	2536.9	40.0	2610.1	7.5	2.8%
05KP30_012a	11.9718	0.2627	0.4947	0.0100	0.1755	0.0009	2602.2	20.4	2591.0	42.9	2611.0	8.1	0.8%
05KP30_013a	11.7866	0.3134	0.4883	0.0121	0.1751	0.0010	2587.6	24.6	2563.4	52.2	2606.6	9.2	1.7%
05KP30_014a	16.0108	0.3704	0.5657	0.0121	0.2053	0.0010	2877.4	21.9	2890.3	49.8	2868.5	7.9	-0.8%
05KP30_015a	25.3162	0.9249	0.6884	0.0241	0.2667	0.0016	3320.5	35.1	3376.6	91.4	3286.8	9.2	-2.7%
05KP30_016a	11.8592	0.2949	0.4924	0.0114	0.1747	0.0009	2593.4	23.0	2581.0	49.2	2603.0	8.4	0.8%
05KP30_017a	6.5941	0.2627	0.3733	0.0136	0.1281	0.0013	2058.6	34.5	2044.7	63.4	2072.5	17.9	1.3%
05KP30_018a	13.3382	0.3081	0.4934	0.0106	0.1961	0.0010	2703.9	21.6	2585.2	45.4	2793.8	8.1	7.5%
05KP30_019a	26.0423	0.7287	0.6786	0.0179	0.2783	0.0015	3348.1	27.0	3339.0	68.3	3353.6	8.4	0.4%
05KP30_020a	7.4295	0.2563	0.4072	0.0129	0.1323	0.0011	2164.5	30.4	2202.3	59.0	2128.9	14.5	-3.4%
05KP30_020b	6.5629	0.2427	0.3714	0.0128	0.1281	0.0011	2054.4	32.1	2036.2	59.7	2072.7	14.9	1.8%
05KP30_021a	12.0876	0.2731	0.4867	0.0102	0.1801	0.0009	2611.2	21.0	2556.6	44.0	2653.9	8.1	3.7%
05KP30_022a	12.9714	0.3222	0.5161	0.0118	0.1823	0.0011	2677.6	23.2	2682.4	50.0	2673.9	9.6	-0.3%
05KP30_024a	11.9080	0.2879	0.4897	0.0111	0.1764	0.0009	2597.2	22.4	2569.3	47.8	2619.1	8.1	1.9%
05KP30_024b	10.8373	0.2887	0.4500	0.0113	0.1746	0.0009	2509.3	24.5	2395.5	50.3	2602.7	8.1	8.0%
05KP30_025a	12.3541	0.3055	0.4997	0.0115	0.1793	0.0010	2631.7	23.0	2612.6	49.1	2646.4	9.0	1.3%
05KP30_026a	15.7651	0.4021	0.5525	0.0133	0.2069	0.0010	2862.7	24.1	2835.6	54.8	2881.7	8.0	1.6%

Sample	$^{207}Pb/^{235}U$ intercept	2σ	$^{206}Pb/^{238}U$ intercept	2σ	$^{207}Pb/^{206}Pb$ average	2σ	$^{207}Pb/^{235}U$ age (Ma)	2σ	$^{206}Pb/^{238}U$ age (Ma)	2σ	$^{207}Pb/^{206}Pb$ age (Ma)	2σ	% discordant
05KP30_027a	12.2672	0.2524	0.4943	0.0093	0.1800	0.0009	2625.1	19.1	2589.2	39.9	2652.9	8.0	2.4%
05KP30_028a	23.4032	0.6318	0.6722	0.0171	0.2525	0.0013	3243.9	26.0	3314.3	65.6	3200.6	8.2	-3.6%
05KP30_029a	11.1008	0.3149	0.4527	0.0120	0.1778	0.0011	2531.6	26.1	2407.4	52.9	2632.8	10.2	8.6%
05KP30_030a	10.7062	0.2628	0.4480	0.0104	0.1733	0.0008	2498.0	22.5	2386.5	46.0	2589.9	7.7	7.9%
05KP30_031a	11.8624	0.3931	0.4871	0.0150	0.1766	0.0013	2593.6	30.6	2558.3	64.7	2621.3	12.2	2.4%
05KP30_033a	10.7796	0.6017	0.4473	0.0240	0.1748	0.0016	2504.3	50.6	2383.2	106.1	2604.0	15.5	8.5%
05KP30_034a	23.8746	0.6021	0.6451	0.0151	0.2684	0.0013	3263.3	24.3	3209.1	59.0	3296.8	7.7	2.7%
05KP30_035b	6.7256	0.2492	0.3772	0.0129	0.1293	0.0012	2076.0	32.2	2063.2	60.0	2088.7	15.7	1.2%
05KP30_036a	16.1983	0.5605	0.5624	0.0184	0.2089	0.0013	2888.6	32.6	2876.7	75.5	2896.9	10.4	0.7%
05KP30_037a	6.4617	0.2172	0.3599	0.0113	0.1302	0.0009	2040.7	29.1	1981.7	53.2	2100.8	12.6	5.7%
05KP30_038a	6.6599	0.2184	0.3723	0.0113	0.1297	0.0010	2067.3	28.5	2040.4	52.9	2094.2	13.0	2.6%
05KP30_040a	27.8168	0.7555	0.6824	0.0173	0.2957	0.0015	3412.7	26.3	3353.5	66.1	3447.6	8.0	2.7%
05KP30_040b	27.9909	0.7551	0.6870	0.0173	0.2955	0.0015	3418.8	26.1	3371.2	65.8	3446.8	8.1	2.2%
05KP30_041a	15.1006	0.4510	0.5339	0.0130	0.2051	0.0018	2821.6	28.1	2757.9	54.5	2867.4	14.2	3.8%
05KP30_042a	11.5501	0.3720	0.4776	0.0128	0.1754	0.0016	2568.6	29.7	2516.9	55.8	2609.7	15.2	3.6%
05KP30_043a	6.9355	0.2899	0.3778	0.0139	0.1331	0.0015	2103.2	36.4	2066.1	64.6	2139.7	19.4	3.4%
05KP30_044a	11.5180	0.6027	0.4819	0.0229	0.1734	0.0022	2566.0	47.8	2535.4	99.0	2590.3	20.8	2.1%
05KP30_045a	12.0464	0.3773	0.4936	0.0128	0.1770	0.0016	2608.0	29.0	2586.2	54.9	2625.0	15.1	1.5%
05KP30_046a	11.5512	0.4071	0.4829	0.0146	0.1735	0.0017	2568.7	32.4	2540.0	63.0	2591.5	16.0	2.0%
05KP30_047a	11.8143	0.3518	0.4831	0.0117	0.1774	0.0016	2589.8	27.5	2540.8	50.6	2628.4	14.6	3.3%
05KP30_048a	12.1779	0.3651	0.4978	0.0122	0.1774	0.0016	2618.2	27.8	2604.3	52.2	2628.9	14.6	0.9%
05KP30_048b	12.2250	0.4006	0.4958	0.0137	0.1788	0.0016	2621.8	30.3	2595.6	58.6	2642.1	15.2	1.8%
05KP30_048c	12.0345	0.3927	0.4722	0.0129	0.1848	0.0017	2607.1	30.1	2493.3	56.0	2696.7	15.5	7.5%
05KP30_050a	12.1087	0.3501	0.4965	0.0115	0.1769	0.0015	2612.9	26.8	2598.6	49.5	2623.9	14.5	1.0%
05KP30_053a	12.4624	0.3655	0.4979	0.0108	0.1815	0.0018	2639.9	27.2	2604.6	46.3	2667.0	16.4	2.3%
05KP30_054a	11.8969	0.4886	0.4935	0.0173	0.1748	0.0020	2596.3	37.8	2585.9	74.3	2604.4	18.7	0.7%

Sample	$^{207}Pb/^{235}U$ intercept	2σ	$^{206}Pb/^{238}U$ intercept	2σ	$^{207}Pb/^{206}Pb$ average	2σ	$^{207}Pb/^{235}U$ age (Ma)	2σ	$^{206}Pb/^{238}U$ age (Ma)	2σ	$^{207}Pb/^{206}Pb$ age (Ma)	2σ	% discordant
05KP30_055a	16.6748	0.4948	0.5841	0.0129	0.2071	0.0021	2916.3	28.0	2965.3	52.4	2882.7	16.1	-2.9%
05KP30_056a	12.5268	0.3659	0.5145	0.0111	0.1766	0.0018	2644.7	27.1	2675.9	46.9	2621.0	16.5	-2.1%
05KP30_057b	11.5187	0.4282	0.4826	0.0148	0.1731	0.0019	2566.1	34.2	2538.6	63.9	2587.9	18.4	1.9%
05KP30_058a	23.7398	0.7112	0.6480	0.0147	0.2657	0.0026	3257.8	28.8	3220.6	57.1	3280.7	15.4	1.8%
05KP30_059a	11.8510	0.3470	0.4909	0.0106	0.1751	0.0017	2592.7	27.1	2574.6	45.9	2606.9	16.4	1.2%
05KP30_060a	11.8951	0.3532	0.4921	0.0109	0.1753	0.0018	2596.2	27.4	2579.7	46.7	2609.1	16.7	1.1%
05KP30_061a	22.7970	0.5909	0.6028	0.0123	0.2743	0.0022	3218.3	24.9	3041.3	49.3	3330.7	12.4	8.7%
05KP30_062a	12.3737	0.3036	0.5067	0.0094	0.1771	0.0014	2633.2	22.8	2642.4	40.1	2626.2	13.4	-0.6%
05KP30_063a	7.7705	0.2359	0.4027	0.0096	0.1399	0.0015	2204.8	26.9	2181.7	43.8	2226.4	18.2	2.0%
05KP30_064a	11.8714	0.4704	0.4930	0.0173	0.1747	0.0017	2594.3	36.4	2583.5	74.2	2602.8	16.2	0.7%
05KP30_065a	27.3856	0.6733	0.6783	0.0127	0.2928	0.0023	3397.4	23.8	3337.8	48.7	3432.7	12.3	2.8%
05KP30_066a	16.1351	0.3884	0.5618	0.0101	0.2083	0.0017	2884.8	22.8	2874.0	41.7	2892.5	12.9	0.6%
05KP30_067a	11.8191	0.2936	0.4950	0.0094	0.1732	0.0014	2590.2	23.0	2592.2	40.4	2588.7	13.4	-0.1%
05KP30_070a	11.3200	0.3033	0.4717	0.0099	0.1741	0.0015	2549.9	24.7	2491.0	43.0	2597.1	14.5	4.1%
05KP30_070b	11.2952	0.3358	0.4702	0.0115	0.1742	0.0015	2547.8	27.4	2484.6	50.3	2598.6	14.4	4.4%
05KP30_071a	15.6732	0.3379	0.5521	0.0088	0.2059	0.0015	2857.1	20.4	2833.9	36.4	2873.5	11.9	1.4%
05KP30_072a	15.5781	0.4084	0.5402	0.0114	0.2092	0.0017	2851.3	24.7	2784.2	47.4	2899.0	13.3	4.0%
05KP30_073a	11.6101	0.3863	0.4805	0.0138	0.1752	0.0016	2573.5	30.6	2529.4	60.0	2608.4	14.8	3.0%
05KP30_074a	11.8056	0.2501	0.4864	0.0075	0.1760	0.0013	2589.1	19.6	2555.1	32.6	2615.8	12.0	2.3%
05KP30_075a	24.4470	0.5238	0.6405	0.0100	0.2768	0.0021	3286.4	20.7	3190.8	39.3	3345.2	11.6	4.6%
05KP30_077a	11.6769	0.2541	0.4753	0.0077	0.1782	0.0013	2578.9	20.2	2506.9	33.6	2635.9	12.1	4.9%
05KP30_078a	11.9778	0.2669	0.4890	0.0082	0.1776	0.0013	2602.7	20.7	2566.4	35.2	2631.0	12.5	2.5%
05KP30_080a	11.6315	0.3004	0.4846	0.0100	0.1741	0.0014	2575.2	23.9	2547.2	43.5	2597.3	13.3	1.9%
05KP30_081a	11.5747	0.2660	0.4787	0.0092	0.1754	0.0012	2570.6	21.3	2521.7	39.8	2609.5	11.3	3.4%
05KP30_082a	11.7156	0.2724	0.4853	0.0094	0.1751	0.0012	2581.9	21.5	2550.1	40.7	2607.0	11.5	2.2%
05KP30_083a	12.3927	0.2675	0.4921	0.0088	0.1827	0.0012	2634.6	20.1	2579.6	37.7	2677.1	10.6	3.6%

Sample	$^{207}Pb/^{235}U$ intercept	2σ	$^{206}Pb/^{238}U$ intercept	2σ	$^{207}Pb/^{206}Pb$ average	2σ	$^{207}Pb/^{235}U$ age (Ma)	2σ	$^{206}Pb/^{238}U$ age (Ma)	2σ	$^{207}Pb/^{206}Pb$ age (Ma)	2σ	% discordant
05KP30_084a	15.7378	0.3063	0.5479	0.0084	0.2083	0.0013	2861.0	18.4	2816.3	35.0	2892.7	10.0	2.6%
05KP30_085a	6.8572	0.1891	0.3825	0.0091	0.1300	0.0010	2093.1	24.1	2087.9	42.4	2098.3	13.6	0.5%
05KP30_086a	11.7954	0.2401	0.4786	0.0079	0.1788	0.0011	2588.3	18.9	2521.1	34.3	2641.3	10.2	4.6%
05KP30_087a	12.2717	0.2653	0.4889	0.0086	0.1820	0.0012	2625.4	20.1	2566.0	37.3	2671.5	11.0	4.0%
05KP30_088a	11.8894	0.2556	0.4866	0.0087	0.1772	0.0011	2595.7	19.9	2556.1	37.5	2626.8	10.3	2.7%
05KP30_089a	15.8367	0.3169	0.5414	0.0087	0.2121	0.0013	2867.0	18.9	2789.3	36.4	2922.0	9.8	4.5%
05KP30_091a	11.7586	0.5958	0.4941	0.0236	0.1726	0.0012	2585.4	46.3	2588.4	100.9	2582.8	11.4	-0.2%
05KP30_092a	11.8952	0.5996	0.4926	0.0234	0.1751	0.0012	2596.2	46.1	2581.9	100.3	2607.2	11.2	1.0%
05KP30_093a	11.2520	0.5987	0.4749	0.0238	0.1718	0.0013	2544.2	48.4	2505.2	103.3	2575.4	12.2	2.7%
05KP30_094a	12.0233	0.6114	0.4966	0.0238	0.1756	0.0012	2606.2	46.6	2599.0	101.6	2611.7	11.6	0.5%
05KP30_096a	11.6518	0.6141	0.4701	0.0232	0.1797	0.0014	2576.8	48.1	2484.0	101.0	2650.5	13.2	6.3%
05KP30_098a	11.9557	0.4149	0.4914	0.0129	0.1764	0.0018	2600.9	32.0	2576.8	55.4	2619.8	17.2	1.6%
05KP30_099a	12.0450	0.4018	0.4973	0.0122	0.1756	0.0018	2607.9	30.8	2602.4	52.2	2612.2	17.1	0.4%
05KP30_100a	6.8989	0.2981	0.3841	0.0137	0.1303	0.0015	2098.5	37.6	2095.4	63.4	2101.6	20.3	0.3%
05KP30_101a	11.5599	0.3992	0.4852	0.0126	0.1728	0.0018	2569.4	31.8	2550.0	54.4	2584.8	17.3	1.3%
05KP30_103a	12.7975	0.4323	0.5172	0.0130	0.1795	0.0018	2664.9	31.3	2687.2	55.0	2647.9	16.9	-1.5%
05KP30_104a	11.6913	0.4023	0.4878	0.0127	0.1738	0.0018	2580.0	31.7	2561.3	54.6	2594.7	17.0	1.3%
05KP30_105a	12.7081	0.4009	0.5011	0.0121	0.1839	0.0018	2658.3	29.3	2618.3	51.5	2688.7	15.7	2.6%
05KP30_106a	11.9871	0.5988	0.5006	0.0222	0.1737	0.0020	2603.4	45.8	2616.2	94.6	2593.4	18.6	-0.9%
05KP30_107a	11.6812	0.3544	0.4863	0.0111	0.1742	0.0016	2579.2	28.0	2554.6	48.0	2598.5	15.2	1.7%
05KP30_108a	11.7487	0.3666	0.4900	0.0116	0.1739	0.0017	2584.6	28.8	2570.8	49.8	2595.3	15.9	0.9%
05KP30_109a	6.6572	0.2520	0.3704	0.0114	0.1304	0.0014	2067.0	32.9	2031.1	53.5	2102.8	18.7	3.4%
05KP30_110a	11.6778	0.3504	0.4902	0.0110	0.1728	0.0016	2578.9	27.7	2571.6	47.3	2584.5	15.3	0.5%
05KP30_112a	11.6346	0.3526	0.4769	0.0108	0.1769	0.0017	2575.5	28.0	2513.8	47.0	2624.3	15.5	4.2%
05KP30_113a	11.5618	0.4201	0.4762	0.0140	0.1761	0.0018	2569.6	33.4	2510.8	60.7	2616.2	17.1	4.0%
05KP30_114a	11.8669	0.3565	0.4913	0.0110	0.1752	0.0016	2594.0	27.7	2576.5	47.3	2607.6	15.4	1.2%

05KP30_115a	11.6167	0.3517	0.4816	0.0109	0.1749	0.0016	2574.0	27.9	2534.3	47.3	2605.3	15.4	2.7%
05KP30_116a	11.5763	0.3974	0.4872	0.0145	0.1723	0.0014	2570.8	31.6	2558.3	62.5	2580.4	13.5	0.9%
05KP30_117a	26.0998	0.8394	0.6709	0.0186	0.2821	0.0021	3350.3	31.0	3309.2	71.5	3374.8	11.5	1.9%
05KP30_118a	22.3742	0.8171	0.6228	0.0201	0.2606	0.0021	3200.1	34.9	3120.9	79.3	3250.0	12.6	4.0%
05KP30_120a	6.6389	0.2554	0.3670	0.0123	0.1312	0.0013	2064.5	33.4	2015.3	57.5	2113.9	16.8	4.7%

> 10% discordant

Sample #	$^{207}Pb/^{235}U$ intercept	2σ	$^{206}Pb/^{238}U$ intercept	2σ	$^{207}Pb/^{206}Pb$ average	2σ	$^{207}Pb/^{235}U$ age	2σ	$^{206}Pb/^{238}U$ age	2σ	$^{207}Pb/^{206}Pb$ age	2σ	% discordant
05KP30_006a	19.7457	0.4799	0.5308	0.0101	0.2698	0.0021	3079.0	23.2	2744.8	42.4	3304.8	12.2	16.9%
05KP30_006b	5.1942	0.3152	0.1459	0.0085	0.2582	0.0022	1851.7	50.4	878.1	47.7	3235.5	13.6	72.9%
05KP30_009a	19.7640	0.4976	0.5522	0.0111	0.2596	0.0020	3079.9	24.0	2834.2	46.1	3244.2	12.1	12.6%
05KP30_023a	20.7594	0.4720	0.5740	0.0120	0.2623	0.0014	3127.4	21.8	2924.3	49.0	3260.5	8.1	10.3%
05KP30_032a	11.2937	0.3139	0.4333	0.0112	0.1890	0.0010	2547.7	25.6	2320.8	50.3	2733.6	9.0	15.1%
05KP30_034b	9.5677	0.5473	0.3332	0.0183	0.2082	0.0021	2394.1	51.3	1854.1	87.7	2891.8	16.5	35.9%
05KP30_035a	7.4491	0.2176	0.3550	0.0095	0.1522	0.0010	2166.9	25.8	1958.4	45.1	2370.6	11.6	17.4%
05KP30_039a	8.7522	0.2607	0.3597	0.0100	0.1765	0.0010	2312.5	26.8	1980.6	47.4	2620.1	9.7	24.4%
05KP30_051a	10.3245	0.3136	0.4226	0.0098	0.1772	0.0018	2464.3	27.7	2272.2	44.2	2626.8	16.3	13.5%
05KP30_052a	10.8507	0.3275	0.3940	0.0088	0.1997	0.0021	2510.4	27.7	2141.3	40.5	2824.1	17.0	24.2%
05KP30_057a	10.6682	0.4733	0.4399	0.0166	0.1759	0.0023	2494.7	40.4	2350.4	74.0	2614.3	21.4	10.1%
05KP30_068a	19.9682	0.4924	0.5537	0.0104	0.2616	0.0021	3089.8	23.6	2840.5	43.1	3256.2	12.5	12.8%
05KP30_069a	12.1519	0.4106	0.4574	0.0131	0.1927	0.0018	2616.2	31.2	2427.9	57.7	2765.4	15.5	12.2%
05KP30_076a	11.4595	0.2598	0.4533	0.0077	0.1833	0.0014	2561.3	21.0	2410.0	34.3	2683.3	12.6	10.2%
05KP30_079a	20.6065	0.4833	0.5300	0.0095	0.2820	0.0022	3120.3	22.5	2741.3	40.1	3374.1	12.0	18.8%
05KP30_090a	5.7023	0.2664	0.2409	0.0092	0.1717	0.0030	1931.7	39.6	1391.5	47.8	2573.8	28.9	45.9%
05KP30_095a	18.4857	1.2404	0.5423	0.0334	0.2472	0.0034	3015.4	62.7	2793.1	138.0	3166.9	21.7	11.8%
05KP30_097a	10.0836	0.8213	0.4226	0.0324	0.1730	0.0021	2442.5	72.6	2272.4	145.3	2587.3	20.1	12.2%
05KP30_102a	6.9936	0.2483	0.2937	0.0077	0.1727	0.0019	2110.6	31.1	1660.0	38.5	2584.0	18.7	35.8%
05KP30_111a	9.8771	0.3172	0.3906	0.0097	0.1834	0.0017	2423.4	29.2	2125.7	45.0	2683.7	15.4	20.8%
05KP30_119a	12.6238	0.4380	0.4672	0.0141	0.1960	0.0016	2652.0	32.1	2471.1	61.5	2792.9	13.4	11.5%

Appendix D: Sample 05KP32

< 10% discordant

Sample #	$^{207}Pb/^{235}U$ intercept	2σ	$^{206}Pb/^{238}U$ intercept	2σ	$^{207}Pb/^{206}Pb$ average	2σ	$^{207}Pb/^{235}U$ age (Ma)	2σ	$^{206}Pb/^{238}U$ age (Ma)	2σ	$^{207}Pb/^{206}Pb$ age (Ma)	2σ	% discordant
05KP32_001a	27.2476	0.9160	0.6613	0.0217	0.2989	0.0019	3392.4	32.4	3272.1	83.6	3464.4	9.6	5.5%
05KP32_006a	12.1337	0.4080	0.4666	0.0153	0.1886	0.0012	2614.8	31.1	2468.6	66.8	2730.2	10.6	9.6%
05KP32_008a	25.0790	0.8482	0.6172	0.0203	0.2947	0.0019	3311.3	32.5	3098.7	80.5	3442.8	10.2	10.0%
05KP32_011a	11.1327	0.1939	0.4501	0.0078	0.1794	0.0006	2534.3	16.1	2395.7	34.4	2647.2	5.5	9.5%
05KP32_018a	10.8533	0.1763	0.4564	0.0065	0.1725	0.0013	2510.6	15.0	2423.5	28.8	2581.9	12.5	6.1%
05KP32_019a	12.0779	0.2029	0.4850	0.0072	0.1806	0.0014	2610.5	15.6	2549.2	31.2	2658.4	12.6	4.1%
05KP32_023a	12.7914	0.2450	0.4756	0.0082	0.1951	0.0016	2664.4	17.9	2507.9	35.8	2785.5	13.7	10.0%
05KP32_024a	10.8417	0.1771	0.4573	0.0066	0.1720	0.0012	2509.6	15.1	2427.4	29.2	2576.9	12.0	5.8%
05KP32_032a	28.2106	0.4072	0.6816	0.0089	0.3002	0.0018	3426.4	14.1	3350.5	34.1	3471.2	9.2	3.5%
05KP32_034a	11.3920	0.1597	0.4712	0.0060	0.1754	0.0010	2555.8	13.0	2488.7	26.0	2609.4	9.9	4.6%
05KP32_034b	12.5808	0.1692	0.5112	0.0061	0.1785	0.0011	2648.8	12.6	2661.8	26.1	2638.9	9.9	-0.9%
05KP32_037a	12.2932	0.1703	0.4980	0.0059	0.1790	0.0013	2627.1	12.9	2605.4	25.1	2643.8	11.8	1.5%
05KP32_038a	12.6204	0.1584	0.4948	0.0050	0.1850	0.0013	2651.7	11.7	2591.4	21.7	2698.1	11.8	4.0%
05KP32_044a	10.3637	0.1278	0.4610	0.0046	0.1631	0.0011	2467.8	11.4	2443.9	20.3	2487.6	11.7	1.8%
05KP32_046a	16.3018	0.3600	0.5406	0.0115	0.2187	0.0014	2894.7	20.9	2786.1	47.9	2971.0	10.6	6.2%
05KP32_048a	12.9256	0.1831	0.5163	0.0067	0.1816	0.0011	2674.2	13.3	2683.6	28.2	2667.1	9.7	-0.6%
05KP32_049a	14.2447	0.2018	0.5218	0.0067	0.1980	0.0012	2766.1	13.4	2706.6	28.4	2809.8	9.8	3.7%
05KP32_051a	13.8810	0.1844	0.5121	0.0061	0.1966	0.0012	2741.6	12.5	2665.6	25.9	2798.0	9.7	4.7%
05KP32_052b	13.4710	0.1771	0.5247	0.0062	0.1862	0.0011	2713.3	12.4	2718.9	26.0	2709.0	9.6	-0.4%
05KP32_053a	6.8798	0.1875	0.3677	0.0098	0.1357	0.0009	2096.1	23.9	2018.5	46.1	2173.0	11.0	7.1%
05KP32_055a	11.3704	0.1538	0.4659	0.0056	0.1770	0.0011	2554.0	12.5	2465.5	24.6	2625.0	10.5	6.1%
05KP32_057a	12.9122	0.2365	0.5052	0.0087	0.1854	0.0013	2673.3	17.1	2636.1	37.2	2701.5	11.3	2.4%
05KP32_059a	16.1300	0.2803	0.5306	0.0086	0.2205	0.0016	2884.5	16.5	2744.1	36.1	2984.1	11.4	8.0%

Sample #	$^{207}Pb/^{235}U$ intercept	2σ	$^{206}Pb/^{238}U$ intercept	2σ	$^{207}Pb/^{206}Pb$ average	2σ	$^{207}Pb/^{235}U$ age (Ma)	2σ	$^{206}Pb/^{238}U$ age (Ma)	2σ	$^{207}Pb/^{206}Pb$ age (Ma)	2σ	% discordant
05KP32_061a	14.3445	0.2653	0.5617	0.0099	0.1852	0.0010	2772.8	17.4	2873.7	40.9	2700.1	9.3	-6.4%
05KP32_062a	7.3518	0.1651	0.4154	0.0090	0.1284	0.0008	2155.1	19.9	2239.4	41.1	2075.7	10.7	-7.9%
05KP32_063a	12.6115	0.1671	0.5084	0.0061	0.1799	0.0011	2651.1	12.4	2649.6	26.0	2652.2	9.7	0.1%
05KP32_065a	8.3012	0.1121	0.4014	0.0049	0.1500	0.0009	2264.5	12.2	2175.3	22.6	2346.0	10.1	7.3%
05KP32_066a	10.9072	0.1297	0.4588	0.0049	0.1724	0.0010	2515.3	11.0	2434.1	21.4	2581.4	9.2	5.7%
05KP32_068a	13.1953	0.2723	0.5220	0.0082	0.1833	0.0024	2693.7	19.3	2707.9	34.7	2683.0	21.2	-0.9%
05KP32_069b	28.4824	0.5760	0.6887	0.0106	0.2999	0.0038	3435.8	19.6	3377.7	40.3	3469.9	19.4	2.7%
05KP32_071a	10.3992	0.2426	0.4683	0.0090	0.1610	0.0021	2471.0	21.4	2476.1	39.4	2466.7	21.4	-0.4%
05KP32_072a	12.5767	0.2452	0.5014	0.0072	0.1819	0.0023	2648.5	18.2	2619.8	31.0	2670.4	20.6	1.9%
05KP32_073a	15.6778	0.4040	0.5393	0.0119	0.2108	0.0028	2857.4	24.3	2780.7	49.6	2911.8	21.0	4.5%
05KP32_074a	28.8551	0.6423	0.7116	0.0128	0.2941	0.0037	3448.6	21.6	3464.3	48.0	3439.4	19.5	-0.7%
05KP32_079a	14.1080	0.3227	0.5087	0.0084	0.2012	0.0030	2757.0	21.5	2650.9	35.6	2835.7	24.4	6.5%
05KP32_080a	10.9662	0.2235	0.4502	0.0057	0.1767	0.0027	2520.3	18.8	2396.4	25.5	2621.7	24.7	8.6%
05KP32_081a	28.1187	0.6195	0.6874	0.0106	0.2967	0.0044	3423.2	21.4	3372.7	40.3	3453.0	22.7	2.3%
05KP32_084a	28.0826	0.7254	0.7170	0.0146	0.2841	0.0042	3422.0	25.0	3484.7	54.7	3385.5	23.1	-2.9%
05KP32_084b	28.5904	0.6128	0.7036	0.0102	0.2947	0.0044	3439.6	20.8	3434.4	38.5	3442.6	22.8	0.2%
05KP32_085a	12.0802	0.2304	0.4821	0.0051	0.1817	0.0027	2610.7	17.7	2536.3	22.2	2668.9	24.5	5.0%
05KP32_086a	28.5691	0.6079	0.6931	0.0099	0.2990	0.0044	3438.8	20.7	3394.3	37.7	3464.9	22.6	2.0%
05KP32_087a	13.4227	0.4420	0.5234	0.0151	0.1860	0.0029	2709.9	30.6	2713.8	63.4	2707.0	25.3	-0.3%
05KP32_088a	12.9121	0.2538	0.5039	0.0059	0.1859	0.0028	2673.3	18.4	2630.5	25.2	2705.8	24.2	2.8%
05KP32_089a	13.3100	0.5358	0.4979	0.0198	0.1939	0.0012	2701.9	37.3	2604.8	84.7	2775.3	10.5	6.1%
05KP32_091a	12.0041	0.1775	0.4757	0.0065	0.1830	0.0011	2604.7	13.8	2508.3	28.2	2680.6	9.5	6.4%
05KP32_093a	28.1753	0.3081	0.6661	0.0063	0.3068	0.0016	3425.2	10.7	3290.8	24.2	3504.8	8.2	6.1%
05KP32_094b	26.6593	0.3690	0.6552	0.0082	0.2951	0.0017	3371.0	13.5	3248.4	31.9	3444.7	9.0	5.7%
05KP32_098a	12.0223	0.2405	0.4867	0.0091	0.1791	0.0013	2606.1	18.6	2556.6	39.4	2644.9	11.8	3.3%

05KP32_100a	13.0179	0.2387	0.5074	0.0086	0.1861	0.0013	2681.0	17.1	2645.7	36.6	2707.7	11.6	2.3%
05KP32_101a	24.2164	0.3361	0.6354	0.0076	0.2764	0.0019	3277.1	13.4	3170.8	29.9	3342.9	10.7	5.1%
05KP32_102b	24.4225	0.7094	0.6346	0.0179	0.2791	0.0021	3285.4	27.9	3167.7	70.2	3358.1	11.7	5.7%
05KP32_103a	26.3966	0.3428	0.6287	0.0070	0.3045	0.0019	3361.3	12.6	3144.5	27.7	3493.4	9.6	10.0%
05KP32_104a	11.8811	0.2210	0.4683	0.0079	0.1840	0.0015	2595.1	17.3	2476.0	34.8	2689.4	13.2	7.9%

> 10% discordant

Sample #	$^{207}Pb/^{235}U$ intercept	2σ	$^{206}Pb/^{238}U$ intercept	2σ	$^{207}Pb/^{206}Pb$ average	2σ	$^{207}Pb/^{235}U$ age (Ma)	2σ	$^{206}Pb/^{238}U$ age (Ma)	2σ	$^{207}Pb/^{206}Pb$ age (Ma)	2σ	% discordant
05KP32_004a	19.9921	0.6662	0.5288	0.0172	0.2742	0.0017	3091.0	31.7	2736.5	72.0	3330.3	9.9	17.8%
05KP32_009a	11.2453	0.3901	0.4149	0.0139	0.1966	0.0017	2543.7	31.8	2237.2	63.0	2798.2	13.7	20.0%
05KP32_012a	15.3610	0.2295	0.4811	0.0069	0.2315	0.0011	2837.9	14.1	2532.3	30.2	3062.8	7.3	17.3%
05KP32_012b	11.1255	0.1765	0.4128	0.0061	0.1955	0.0014	2533.7	14.7	2227.6	27.6	2788.8	11.4	20.1%
05KP32_014b	12.5627	0.1952	0.4472	0.0061	0.2037	0.0014	2647.4	14.5	2382.9	27.2	2856.3	11.2	16.6%
05KP32_015a	15.6198	0.2053	0.5094	0.0065	0.2224	0.0008	2853.8	12.5	2654.0	27.8	2998.1	5.7	11.5%
05KP32_016b	9.1497	0.1652	0.3504	0.0056	0.1894	0.0016	2353.1	16.4	1936.5	26.8	2736.9	13.7	29.2%
05KP32_020a	22.8695	0.4584	0.5380	0.0099	0.3083	0.0025	3221.4	19.3	2775.0	41.3	3512.5	12.3	21.0%
05KP32_024b	8.7864	0.1749	0.3703	0.0067	0.1721	0.0015	2316.1	18.0	2030.8	31.3	2578.1	14.5	21.2%
05KP32_025a	13.2712	0.1965	0.4213	0.0056	0.2285	0.0015	2699.1	13.9	2266.3	25.4	3041.4	10.5	25.5%
05KP32_026a	12.3193	0.1843	0.4558	0.0061	0.1960	0.0013	2629.0	14.0	2420.8	27.1	2793.5	10.8	13.3%
05KP32_027a	21.1822	0.2797	0.4797	0.0057	0.3203	0.0018	3147.0	12.7	2526.0	24.6	3571.1	8.7	29.3%
05KP32_030a	8.7079	0.1184	0.3611	0.0043	0.1749	0.0012	2307.9	12.3	1987.6	20.3	2604.9	11.3	23.7%
05KP32_033a	12.6943	0.1783	0.4059	0.0050	0.2268	0.0015	2657.2	13.1	2196.0	23.0	3029.9	10.8	27.5%
05KP32_040a	12.8414	0.1622	0.4740	0.0049	0.1965	0.0013	2668.1	11.8	2501.2	21.5	2797.1	11.2	10.6%
05KP32_042a	9.3146	0.1859	0.4039	0.0075	0.1672	0.0012	2369.5	18.1	2187.2	34.4	2530.2	11.9	13.6%
05KP32_043a	10.4377	0.2040	0.4267	0.0077	0.1774	0.0013	2474.4	17.9	2290.9	34.8	2628.8	12.1	12.9%
05KP32_047a	6.0000	0.0918	0.2970	0.0041	0.1465	0.0010	1975.8	13.2	1676.3	20.6	2305.7	11.3	27.3%
05KP32_050a	10.5628	0.1432	0.4079	0.0049	0.1878	0.0012	2485.4	12.5	2205.4	22.4	2722.9	10.9	19.0%
05KP32_052a	8.1006	0.1593	0.2817	0.0053	0.2085	0.0014	2242.3	17.6	1600.0	26.4	2894.2	10.7	44.7%
05KP32_056a	12.3325	0.2250	0.4529	0.0076	0.1975	0.0016	2630.1	17.0	2408.1	33.7	2805.6	13.5	14.2%
05KP32_058a	6.2178	0.0865	0.2854	0.0036	0.1580	0.0010	2007.0	12.1	1618.4	18.0	2434.5	10.7	33.5%
05KP32_064a	14.2438	0.2219	0.4766	0.0069	0.2168	0.0014	2766.1	14.7	2512.2	30.0	2956.9	10.1	15.0%
05KP32_067a	9.9310	0.1281	0.4156	0.0049	0.1733	0.0010	2428.4	11.8	2240.5	22.1	2589.8	9.3	13.5%

Sample #	$^{207}Pb/^{235}U$ intercept	2σ	$^{206}Pb/^{238}U$ intercept	2σ	$^{207}Pb/^{206}Pb$ average	2σ	$^{207}Pb/^{235}U$ age (Ma)	2σ	$^{206}Pb/^{238}U$ age (Ma)	2σ	$^{207}Pb/^{206}Pb$ age (Ma)	2σ	% discordant
05KP32_069a	10.8437	0.2945	0.3032	0.0072	0.2594	0.0034	2509.8	24.9	1707.2	35.4	3242.8	20.5	47.4%
05KP32_070a	17.9385	0.3930	0.5331	0.0093	0.2440	0.0031	2986.4	20.9	2754.5	39.2	3146.5	19.9	12.5%
05KP32_076a	30.9827	0.6704	0.6464	0.0110	0.3476	0.0045	3518.5	21.1	3213.9	43.0	3696.7	19.5	13.1%
05KP32_077a	16.5162	0.4344	0.5249	0.0119	0.2282	0.0029	2907.2	24.9	2719.8	50.3	3039.5	20.4	10.5%
05KP32_078a	6.4474	0.1418	0.3341	0.0058	0.1399	0.0019	2038.7	19.1	1858.4	28.0	2226.4	22.8	16.5%
05KP32_082a	11.2968	0.2425	0.4458	0.0065	0.1838	0.0027	2547.9	19.8	2376.5	28.8	2687.4	24.4	11.6%
05KP32_090a	17.3249	0.4659	0.4402	0.0115	0.2855	0.0018	2953.0	25.5	2351.3	51.4	3393.1	9.6	30.7%
05KP32_092a	10.5285	0.1888	0.4103	0.0070	0.1861	0.0011	2482.4	16.5	2216.4	31.7	2708.0	9.4	18.2%
05KP32_094a	20.5443	0.2320	0.5421	0.0053	0.2748	0.0015	3117.3	10.9	2792.4	22.0	3333.8	8.8	16.2%
05KP32_096b	19.9685	1.4323	0.3895	0.0278	0.3718	0.0028	3089.8	67.1	2120.6	127.8	3798.8	11.6	44.2%
05KP32_099a	13.1550	0.2297	0.4180	0.0066	0.2283	0.0018	2690.8	16.3	2251.4	29.7	3039.9	12.8	25.9%
05KP32_101b	23.6671	0.3493	0.5775	0.0075	0.2972	0.0020	3254.8	14.3	2938.7	30.6	3455.8	10.6	15.0%
05KP32_105a	17.0826	0.3488	0.4588	0.0088	0.2700	0.0019	2939.5	19.4	2434.3	38.8	3306.3	11.0	26.4%
05KP32_106a	13.5836	0.2173	0.3766	0.0054	0.2616	0.0018	2721.1	15.0	2060.6	25.3	3256.2	10.8	36.7%

207/206 only

Sample #	$^{207}Pb/^{235}U$ intercept	2σ	$^{206}Pb/^{238}U$ intercept	2σ	$^{207}Pb/^{206}Pb$ average	2σ	$^{207}Pb/^{235}U$ age (Ma)	2σ	$^{206}Pb/^{238}U$ age (Ma)	2σ	$^{207}Pb/^{206}Pb$ age (Ma)	2σ	% discordant
05KP32_001b	21.8350	1.3902	0.4896	0.0309	0.3235	0.0025	3176.4	60.0	2568.8	132.4	3586.6	11.6	28.4%
05KP32_001c	19.7767	0.7848	0.4757	0.0185	0.3016	0.0019	3080.5	37.6	2508.4	80.5	3478.3	9.9	27.9%
05KP32_002a	10.9960	1.6721	0.4065	0.0618	0.1962	0.0016	2522.8	132.5	2199.1	277.1	2794.7	13.3	21.3%
05KP32_003a	10.1305	0.4124	0.4105	0.0164	0.1790	0.0012	2446.8	36.9	2217.0	74.6	2643.9	11.0	16.1%
05KP32_005a	11.9737	0.4167	0.4404	0.0149	0.1972	0.0015	2602.3	32.1	2352.2	66.3	2803.4	12.1	16.1%
05KP32_007a	15.5853	0.5539	0.4466	0.0154	0.3100	0.0019	2851.7	33.4	2380.3	68.4	3520.9	9.3	32.4%
05KP32_010a	8.0880	0.5397	0.2982	0.0198	0.1967	0.0014	2240.9	58.6	1682.3	97.4	2799.3	11.8	39.9%
05KP32_013a	10.0309	0.2692	0.4076	0.0109	0.1785	0.0007	2437.6	24.5	2204.0	49.7	2638.8	6.8	16.5%
05KP32_013b	11.6900	0.4461	0.4594	0.0176	0.1846	0.0008	2579.9	35.1	2436.7	77.1	2694.4	7.1	9.6%
05KP32_014a	12.0425	1.3687	0.4712	0.0539	0.1854	0.0010	2607.7	101.3	2488.8	231.9	2701.4	9.2	7.9%
05KP32_017a	12.9245	0.3211	0.4303	0.0102	0.2178	0.0016	2674.2	23.1	2307.1	45.7	2964.8	12.2	22.2%
05KP32_021a	10.1478	0.4846	0.4405	0.0208	0.1671	0.0012	2448.3	43.2	2353.0	92.5	2528.5	12.3	6.9%
05KP32_028a	22.6886	1.1951	0.5499	0.0287	0.2993	0.0020	3213.7	50.0	2824.6	118.3	3466.5	10.5	18.5%
05KP32_029a	16.7987	0.2660	0.6127	0.0089	0.1989	0.0012	2923.4	15.1	3080.7	35.6	2816.9	9.9	-9.4%
05KP32_031a	14.7686	0.2318	0.5889	0.0085	0.1819	0.0011	2800.4	14.8	2985.1	34.5	2670.1	9.8	-11.8%
05KP32_035a	12.9293	0.2436	0.5260	0.0091	0.1783	0.0013	2674.5	17.6	2724.4	38.5	2637.0	12.0	-3.3%
05KP32_036a	11.3957	0.2567	0.4184	0.0089	0.1975	0.0014	2556.1	20.8	2253.3	40.4	2805.9	11.9	19.7%
05KP32_039a	7.6646	0.2451	0.3646	0.0114	0.1525	0.0012	2192.5	28.3	2004.0	53.5	2373.7	12.8	15.6%
05KP32_039b	8.4137	0.8138	0.3843	0.0372	0.1588	0.0013	2276.7	84.2	2096.2	170.9	2442.9	14.3	14.2%
05KP32_045a	14.5132	0.2612	0.5737	0.0094	0.1835	0.0013	2783.9	17.0	2923.0	38.6	2684.6	11.8	-8.9%
05KP32_046b	20.8531	0.7403	0.5036	0.0176	0.3003	0.0023	3131.8	33.8	2629.2	75.1	3471.9	12.0	24.3%
05KP32_054a	14.6839	0.5535	0.4381	0.0164	0.2431	0.0016	2795.0	35.2	2341.9	73.0	3140.4	10.3	25.4%
05KP32_054b	8.6703	0.8362	0.4950	0.0479	0.1270	0.0010	2304.0	84.2	2592.4	203.2	2057.2	14.1	-26.0%
05KP32_083a	11.9864	0.9818	0.4922	0.0396	0.1766	0.0027	2603.3	74.0	2580.0	169.0	2621.6	25.5	1.6%

05KP32_094c	19.3379	0.3654	0.4781	0.0083	0.2934	0.0022	3058.8	18.1	2519.1	36.2	3435.5	11.8	26.7%
05KP32_097a	4.2783	0.8756	0.1424	0.0292	0.2179	0.0015	1689.2	155.8	858.1	162.4	2965.4	11.1	71.1%
05KP32_102a	14.6121	0.6348	0.4959	0.0213	0.2137	0.0017	2790.3	40.5	2596.4	91.1	2933.8	12.9	11.5%

Appendix E: Sample 05KP36

> 10% discordant

Sample #	$^{207}Pb/^{235}U$ intercept	2σ	$^{206}Pb/^{238}U$ intercept	2σ	$^{207}Pb/^{206}Pb$ average	2σ	$^{207}Pb/^{235}U$ age (Ma)	2σ	$^{206}Pb/^{238}U$ age (Ma)	2σ	$^{207}Pb/^{206}Pb$ age (Ma)	2σ	% discordant
05KP36_001a	3.8381	0.0914	0.2355	0.0051	0.1182	0.0007	1600.8	19.0	1363.1	26.8	1929.5	9.9	29.4%
05KP36_001b	3.6059	0.0763	0.2172	0.0042	0.1204	0.0006	1550.8	16.7	1267.2	22.1	1962.1	8.8	35.4%

Appendix F: Sample 05KP33

Sample	KP05-33a	KP05-33b	KP05-33c
SiO_2	52.83	52.7	52.9
TiO_2	1.08	1.07	1.08
Al_2O_3	14.59	14.61	14.8
FeO	5.12	5.11	5.41
MnO	0.16	0.15	0.15
MgO	3.57	3.63	3.76
CaO	9.87	9.83	9.42
Na_2O	7.1	7.1	7.05
K_2O	0.14	0.1	0.14
P_2O_5	0.15	0.14	0.15
Rb	2	2	2
Ba	158	140	154
Sr	100	90	94
V	136	146	140
Cr	358	360	356
Ni	305	322	317
Zr	74	76	74
Sc	21	22	21
Cu	25	41	43
Co	52	54	55
Zn	68	73	71
Ga	13	14	14
Y	20	20	20
Nb	17	17	17
La	15	16	16
Ce	28	31	30
Th	4	4	4
U	3	3	3
Pb	5	4	5